FACULTY OF SCIENCE
PALACKY UNIVERSITY OLOMOUC

Department of Optics

ADAPTIVE SUBTRACTION OF A SINGLE PHOTON FROM A STATE OF LIGHT

BACHELOR THESIS

Jan Provazník

2015

PŘÍRODOVĚDECKÁ FAKULTA
UNIVERZITA PALACKÉHO V OLOMOUCI

Katedra optiky

ADAPTIVNÍ ODEČTENÍ JEDNOHO FOTONU ZE STAVU SVĚTLA

BAKALÁŘSKÁ PRÁCE

Jan Provazník

2015

FACULTY OF SCIENCE
PALACKY UNIVERSITY OLOMOUC

Department of Optics

ADAPTIVE SUBTRACTION OF A SINGLE PHOTON FROM A STATE OF LIGHT

BACHELOR THESIS

Author	Jan Provazník
Study programme	B1701 Physics
Study branch	General Physics and Mathematical Physics
Study form	daily
Supervisor	Mgr. Petr Marek, Ph.D.

PŘÍRODOVĚDECKÁ FAKULTA
UNIVERZITA PALACKÉHO V OLOMOUCI

Katedra optiky

ADAPTIVNÍ ODEČTENÍ JEDNOHO FOTONU ZE STAVU SVĚTLA

BAKALÁŘSKÁ PRÁCE

Vypracoval	Jan Provazník
Studijní program	B1701 Fyzika
Studijní obor	Obecná fyzika a matematická fyzika
Form studia	prezenční
Vedoucí práce	Mgr. Petr Marek, Ph.D.

Prohlašuji, že jsem bakalářskou diplomovou práci vypracoval samostatně pod dohledem vedoucího práce a za použití uvedených literárních pramenů.

Souhlasím s použitím výsledků práce pro výzkumné účely.

V Olomouci dne 12. 05. 2015

Abstract

The single photon subtraction is an operation commonly employed in production of non–Gaussian states of light. Its primary disadvantage lies in its limited probability of success. In this thesis, we propose a modification of the method, addressing this drawback. The proposed enhancement relies on chaining the individual single photon subtraction operations in a repeat–until–success fashion. We analyze the benefits of this iterative approach using the overall probability of success and the negativity of the successfully subtracted states. We present a significant increase of the success rates for obtaining maximally non–Gaussian states.

Keywords

continuous variables quantum optics, continuous variables quantum information theory, single photon subtraction, squeezed states, non-Gaussian states, adaptive operations

Abstrakt

Odebrání jednoho fotonu je běžně užívanou operací při přípravě ne–Gaussovských stavů světla, jejíž hlavní nevýhodou je omezená pravděpodobnost úspěchu. Navrhovaná úprava zaměřující se na tento problém spočívá v zřetězení jednotlivých odebíracích procedur ve smyslu opakuj–dokud–neuspěješ. Výhody takovéhoto iterativního přístupu jsou analyzovány s pomocí celkové pravděpodobnosti úspěchu a negativity stavů, ze kterých byl foton úspěšně odebrán. Významné zvýšení pravděpodobnosti úspěchu při získání stavů s nejvyšší dosažitelnou negativitou je představeno.

Klíčová slova

spojité proměnné v kvantové optice, spojité proměnné v kvantové teorii informací, odebrání jednoho fotonu, stlačené stavy, ne-Gausovské stavy, adaptivní operace

Acknowledgements

First and foremost, I would like to thank my supervisor Mgr. Petr Marek, Ph.D. for his kind support, never ending guidance and his seemingly unexceedable patience with my perpetual inquiries and glaring lack of any experience whatsoever on my end.

I would also like to express my gratitude to my parents for their financial support of my efforts.

Last but not least, I would like to thank my dear companion Elwin for her passion, beauty and apparently boundless love.

Contents

List of Figures

Introduction

In the recent years the quantum optics has come quite a long way to play an important role in the field of quantum information theory mainly due to its accessibility in experimental implementations of various theoretical concepts [1].

One of the interesting aspects of light is its relative resilience to decoherence. However, the very same property is its greatest shortcoming as it makes most physical interactions nearly impossible, especially on the level of individual photons. As a consequence, fields of light may only be manipulated with linear optical elements, either passive or active, comprising a subset of Gaussian operations. Unfortunately such operations are not applicable in many interesting concepts of quantum information theory, e.g, universal quantum computation [2], entanglement distillation [3], as these require at least cubic non–linear operations [1, 4].

A lot of attention has been therefore dedicated to finding non–Gaussian operations and methods of preparation of non–Gaussian states with a degree of success, as methods such as projective measurements on number states [5, 6], single photon addition [7, 8] and subtraction [9, 10, 11, 12] have been successfully implemented to yield highly non–Gaussian states of light.

In this thesis an improved version of the single photon subtraction procedure [9, 10] is proposed with the intention of enhancing the general performance of the procedure along with the probability of a successful subtraction of a single photon.

In chapter I of the thesis, the necessary theoretical framework is briefly introduced. In chapter II a theoretical model of the original single step subtraction procedure [9] is derived both in the general quantum notation and the phase space representation. Consequently the improved iterative subtraction procedure is introduced in detail in chapter III, where it is also accompanied by a thorough

analysis of mathematical properties of the conclusions arising from phase space description of the iterative procedure.

The effects of both the single step and the iterative procedures on the class of squeezed states of light are compared in chapter IV in terms of the overall success probability and negativity of the resulting non–Gaussian state.

The notation and used symbols

There are quite many different symbols used in this thesis. The rather standard Dirac notation [13] of kets and bras is adopted to describe general quantum states. The Hermitian conjugate operation is denoted using the † (dagger) symbol. In this respect, the symbol ϱ is almost exclusively used for density operators, $\mathbb{1}$ always indicates an identity operator, x and p represent the equivalents of position and momentum operators.

However, x and p can also refer to quadrature variables in the phase spece description, where such entities are often collected in column vectors denoted using $\xi = (x_1, p_1, \ldots, x_\chi, p_\chi)^\intercal$. The symbol ξ_χ then always refers to the $(x_\chi, p_\chi)^\intercal$ subset of the vector ξ.

Gaussian states are characterized by vectors of mean values μ and variance matrices σ. In the current consideration, the variance matrices of the initial and resulting Gaussian states are exclusively diagonal, i.e, $\sigma = \mathrm{diag}\,(\nu_1, \nu_2, \ldots)$.

Wigner functions of general operators ϱ are denoted with the symbol W_ϱ and Gaussian Wigner functions of zero vectors of mean values are expressed as $G\,(\xi, \sigma)$ using their respective variance matrices.

Finally, $\mathbb{I}$ indicates the identity 2×2 matrix and $\mathbb{O}$ a 2×2 matrix of zeroes.

Chapter I

A brief overview of the essential theoretical framework

1 Continuous variables

Traditionally a pair of distinct approaches is used in the quantum information theory. On one hand, observables of discrete spectra, e.g., polarization states or excitation levels of atomic ensembles, are used to encode the information in a digital manner. On the other hand, observables of continuous spectra, e.g., position or momentum of a particle, are used in an analogue manner. The latter approach is commonly referred to as the quantum information theory with continuous variables [14, 4].

An arbitrary quantum system is called a continuous variable system if the dimension of the associated Hilbert state space is infinite [14, 15]. A typical continuous variable system prevalent in the scope of quantum optics is the quantised electromagnetic field, which might be modelled as a collection of one dimensional non–interacting quantum harmonic oscillators with different oscillation frequencies. Each individual oscillator is usually referred to as an oscillation mode of the underlying electromagnetic field or only as a mode for short [1, 15]. Only single oscillatory modes are considered in the context of this thesis.

The quantum state of each oscillatory mode of the field can be naturally described in the number representation, i.e., expressed in the basis of eigen-

states $\{|n\rangle\}$ of the number operator $n = a^\dagger a$ comprising the creation $a^\dagger$ and annihilation a operators of the field excitation. Alternatively the state may be described in the wave function representation [14, 16] employing the eigenstates $\{|x\rangle\}$ of the position operator x, which can be together with the momentum operator p obtained in the form of a combination of the creation and annihilation operators

$$x = \frac{a + a^\dagger}{\sqrt{2}}\,, \quad p = \frac{a - a^\dagger}{\sqrt{-2}} \tag{I.1}$$

adhering to the canonical commutation relation $[x, p] = \imath$.

2 Phase space representation, Wigner distribution functions

The concept of a phase space description is widely employed in the classical statistical physics to characterize physical systems by probability distributions. The probability of finding a physical system in a certain state is then given by the probability distribution in question [17]. This approach, however, can not be directly transcribed to the context of quantum mechanics due to the uncertainty relations arising from the exclusive nature of the physical quantities (position, momentum) used to characterize the physical system.

This issue is quite elegantly resolved with the introduction of quasiprobability distributions [14, 15], which relax some of the Kolmogorov axioms [18]. Although the quasiprobability distributions share some mathematical properties with the classical probability distributions, there are several major differences, such as the possibility of attaining negative values or being singular.

A Wigner distribution functions

Even though there are different quasiprobability distribution functions utilized in the phase space representation of quantum states, only the Wigner distribution function [14, 15, 19] is introduced in this chapter.

Wigner function associated with an arbitrary quantum state of a single mode of light characterized by the density operator ϱ is obtained by employing Wigner's

transformation formula

$$W_{\varrho}(x,p) = \frac{1}{\pi} \int_{-\infty}^{+\infty} \exp(2\imath pq) \, \langle x-q \,|\, \varrho \,|\, x+q \rangle \, \mathrm{d}q \,. \tag{I.2}$$

Some of the more interesting mathematical properties of Wigner functions [14, 15] include (i) — (iv).

(i) Wigner functions are real for Hermitian operators ψ,

$$W_{\varrho}(x,p) \in \mathbb{R} \quad \forall \varrho \in \left\{ \, \varrho \;\middle|\; \varrho = \varrho^{\dagger} \, \right\} \,. \tag{I.3}$$

(ii) Wigner functions are normalized,

$$\int_{-\infty}^{+\infty} \int_{-\infty}^{+\infty} W_{\varrho}(x,p) \, \mathrm{d}x \, \mathrm{d}p = 1 \,. \tag{I.4}$$

(iii) Marginal probability distributions are obtained in the usual manner,

$$\begin{aligned} \langle x \,|\, \varrho \,|\, x \rangle &= \int_{-\infty}^{+\infty} W_{\varrho}(x,p) \, \mathrm{d}p \,, \\ \langle p \,|\, \varrho \,|\, p \rangle &= \int_{-\infty}^{+\infty} W_{\varrho}(x,p) \, \mathrm{d}x \,. \end{aligned} \tag{I.5}$$

(iv) Wigner functions of physical states are bound,

$$|W_{\varrho}(x,p)| \leq \pi^{-1} \,. \tag{I.6}$$

An overlap of two arbitrary operators ϱ, ψ may be obtained using the overlap formula

$$\mathrm{Tr}\,(\varrho\psi) = 2\pi \int_{-\infty}^{+\infty} \int_{-\infty}^{+\infty} W_{\varrho}(x,p) \, W_{\psi}(x,p) \, \mathrm{d}x \, \mathrm{d}p \,, \tag{I.7}$$

which is one of the most remarkable properties of Wigner functions [15] and may be used in a variety of applications, e.g., to obtain transition probabilities and the

purity of quantum ensembles. Similarly, the respective statistical moments

$$\begin{aligned} \mu_n(x) &= \int_{-\infty}^{+\infty}\int_{-\infty}^{+\infty} W_\varrho\,(x,p)\,x^n\;\mathrm{d}x\;\mathrm{d}p\,, \\ \mu_n(p) &= \int_{-\infty}^{+\infty}\int_{-\infty}^{+\infty} W_\varrho\,(x,p)\,p^n\;\mathrm{d}x\;\mathrm{d}p \end{aligned} \tag{I.8}$$

of the quadrature operators x and p may be derived using (I.5). Wigner's formula (I.2) may be extended [14, 4] to apply to multimode product states

$$W_\varrho\,(\xi) = \frac{1}{\pi^\chi}\int_{-\infty}^{+\infty}\cdots\int_{-\infty}^{+\infty} \exp\left(2\imath p\cdot q\right)\left\langle x-q\,\middle|\,\varrho\,\middle|\,x+q\right\rangle\;\mathrm{d}q_1\cdots\mathrm{d}q_\chi\,, \tag{I.9}$$

where $x,p,q\in\mathbb{R}^\chi$ with the integer $\chi\in\mathbb{N}$ denoting the number of modes in the system. The vector $\xi=(x_1,p_1,\ldots,x_\chi,p_\chi)^\intercal\in\mathbb{R}^{2\chi}$ comprises the quadrature variables of individual modes.

The previously obtained properties (i) — (iv) hold even for multimode (multipartite) Wigner functions with minor adjustments of the integration variables. The overlap formula (I.7) can be also adopted to represent partial overlaps

$$\mathrm{Tr}_\chi\left(\varrho\psi\right) = 2\,\pi\int_{-\infty}^{+\infty}\int_{-\infty}^{+\infty} W_\varrho\,(\xi)\,W_\psi\,(\xi)\;\mathrm{d}x_\chi\;\mathrm{d}p_\chi \tag{I.10}$$

where χ refers to the mode the partial overlap is performed over.

B Wigner functions of pure number states

It is only appropriate to derive Wigner functions of pure number states, which were briefly introduced in the section I.1. An arbitrary number state $|n\rangle$ may be obtained [15, 16] by applying the creation operator $a^\dagger$ to the vacuum state $|0\rangle$

$$|n\rangle = \frac{(a^\dagger)^n}{\sqrt{n!}}\,|0\rangle\;. \tag{I.11}$$

The respective Wigner function is then derived [15, 20] using the transformation formula (I.2), yielding a

$$W_{|n\rangle\langle n|}(x,p)\frac{1}{2\pi}L_n\left(x^2+p^2\right)(-1)^n\exp\left(-2^{-1}(x^2+p^2)\right)\,, \tag{I.12}$$

where $L_n(u)$ represents Laguerre polynomial [21] of the order n.

3 Gaussian states and Gaussian operations in the continuous variable quantum optics

Gaussian states [1, 2] are relevant in the continuous variable quantum optics, as such states are produced by some of the most common sources of electromagnetic radiation, such as lasers or black bodies. The class of Gaussian states includes but is not limited to coherent states, thermal states and even the vacuum state $|0\rangle$ related to vacuum fluctuations.

The eventual Gaussian nature of interacting states is preserved by Gaussian operations, which include some of the most common optical elements used to manipulate light, e.g., two mode beam spliterrs, phase shifters and both the single and two mode squeezers [15, 1, 14].

A Gaussian states

An arbitrary multipartite quantum state characterized by the density operator ϱ is a **Gaussian state** if and only if the corresponding Wigner function W_ϱ is found in the form of a Gaussian distribution

$$W_\varrho(\xi)=\frac{1}{(2\pi)^\chi\sqrt{\det(\sigma)}}\exp\left(-\frac{1}{2}(\xi-\mu)^\intercal\sigma^{-1}(\xi-\mu)\right)\,, \tag{I.13}$$

where $\xi,\mu\in\mathbb{R}^{2\chi}$, $\sigma\in\mathbb{R}^{2\chi\times 2\chi}$ with χ indicating the number of optical modes and the vector $\xi=(x_1,p_1,\ldots,x_\chi,p_\chi)^\intercal$ comprises the quadrature variables pertaining to the individual modes similarly to (I.9).

The symbols σ and μ in (I.13) represent the variance matrix and the vector of mean values of the multipartite Gaussian distribution. A Gaussian state is there-

fore completely characterized by the first two moments, μ and σ of the quadrature operators. In this document every Gaussian Wigner function (I.13) with zero vector of mean values $\mu = 0$ is denoted by symbol $G(\xi, \sigma)$

$$G(\xi, \sigma) = \frac{1}{(2\pi)^{\chi}\sqrt{\det(\sigma)}} \exp\left(-\frac{1}{2}\xi^{\intercal}\sigma^{-1}\xi\right) . \tag{I.14}$$

A prime example of a Gaussian state is the vacuum state $|0\rangle$ with the respective Wigner function

$$W_{|0\rangle\langle 0|}(x, p) = \pi^{-1} \exp\left(-x^2 - p^2\right) = G\left((x, p)^{\intercal}, \sigma\right) , \tag{I.15}$$

where $\sigma = \mathrm{diag}(2^{-1}, 2^{-1})$ and $\mu = 0$.

B Gaussian operations

Interactions in quantum optics are generally described using unitary transformations, which might preserve the eventual Gaussian nature of the interacting states of light. Transformations of this kind — labeled **Gaussian operations** — are associated with at most quadratic interaction Hamiltonians in respect to the creation and annihilation operators of the field excitation, therefore affecting at most a pair of modes of light [1, 14].

It is possible to express every Gaussian operation applied on a Gaussian state in the form of a linear transformation V of the coordinate system in the phase space representation, essentially ensuing in the linear transformation

$$\sigma \to V\sigma V^{\intercal} , \quad \mu \to V\mu \tag{I.16}$$

of the respective variance matrix σ and the vector of mean values μ of the Gaussian state [1, 14]. Gaussian operations include linear optical elements such as the single mode squeezer with 2×2 transformation matrix

$$V(\gamma) = \begin{pmatrix} \gamma & 0 \\ 0 & \gamma^{-1} \end{pmatrix} , \tag{I.17}$$

where the parameter γ specifies the squeezing gain (with the momentum p squeezed

for $\gamma > 1$) and the two mode beam splitter with 4×4 transformation matrix

$$V(\zeta) = \begin{pmatrix} \sqrt{\zeta} & 0 & \sqrt{1-\zeta} & 0 \\ 0 & \sqrt{\zeta} & 0 & \sqrt{1-\zeta} \\ \sqrt{1-\zeta} & 0 & \sqrt{\zeta} & 0 \\ 0 & \sqrt{1-\zeta} & 0 & \sqrt{\zeta} \end{pmatrix}, \tag{I.18}$$

where the parameter ζ denotes its transmittance [1, 14, 15].

4 Measurement

One of the most general approaches used to describe measurement operations in quantum physics uses the **positive operator valued measure** [1, 14] composed of Hermitian positive operators (elements) Π^γ corresponding to possible measurement outcomes, where the operators Π^γ add up to an identity operator $\mathbb{1}$.

A measurement operation with the outcome Π^γ performed on the mode χ of a multimode system characterized by the density operator ϱ yields a marginal density operator

$$\varrho' = \mathrm{Tr}_\chi \left[\Pi^\gamma \varrho\right] \left(\mathrm{Tr}\left[\Pi^\gamma \varrho\right]\right)^{-1} \tag{I.19}$$

normalized with the probability of actually measuring the outcome Π^γ given by

$$P_\gamma = \mathrm{Tr}\left[\Pi^\gamma \varrho\right] . \tag{I.20}$$

The positive operator valued measure framework may be adopted in the phase space representation with the aid of Wigner's formula (I.9) and the remarkable overlap formula (I.10), yielding

$$\begin{aligned} W^\gamma_{\varrho'}(\xi') &= (P_\gamma)^{-1} 2\pi \int_{-\infty}^{+\infty}\int_{-\infty}^{+\infty} W_\varrho(\xi)\, W_{\Pi^\gamma}(\xi)\, \mathrm{d}x_\chi\, \mathrm{d}p_\chi , \\ P_\gamma &= 2\pi \int_{-\infty}^{+\infty}\int_{-\infty}^{+\infty} \cdots \int_{-\infty}^{+\infty}\int_{-\infty}^{+\infty} W_\varrho(\xi)\, W_{\Pi^\gamma}(\xi)\, \mathrm{d}x_1\, \mathrm{d}p_1 \cdots \mathrm{d}x_\chi\, \mathrm{d}p_\chi , \end{aligned} \tag{I.21}$$

where the vectors $\xi = (x_1, p_1, \ldots, x_\chi, p_\chi)^\intercal$ and $\xi = (x_1, p_1, \ldots, x_{\chi-1}, p_{\chi-1})^\intercal$ comprise the respective quadrature variables.

Chapter II

Single step single photon subtraction procedure

The single step single photon subtraction procedure was originally conceived and implemented [9] as a method of constructing non–Gaussian states of light. Both the procedure itself and states transformed with the procedure were later on assessed from a theoretical point of view [10]. The subtraction protocol was also utilized in an experimental setting to increase the entanglement between Gaussian states [11] and applied to arbitrary fields of light [12] prepared both in Gaussian and strictly non–Gaussian states.

1 Breakdown of the procedure

The single photon subtraction is realized by reflecting a fragment of the signal mode of light on a strongly unbalanced beam splitter and measuring the reflected fragment of light in the idler mode on an avalanche photodiode. The subtraction is considered **successful** if and only if the detector produces the positive detection outcome, that is if it clicks.

A Ideal detection regime

The conceptual scheme of the subtraction presented in Figure II.1 is divided into three parts, each pertaining to a different logical step of the procedure: a prepara-

tion of both the signal and idler modes (1), tapping off a fraction of the signal mode (2) and finally measuring the idler mode utilizing an ideal avalanche photodiode in (3).

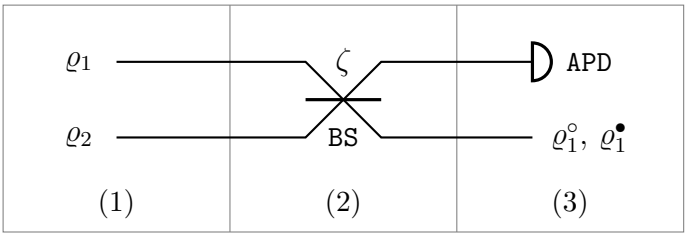

Figure II.1: The procedure transforms the initial signal mode density operator ϱ_1 into either $\varrho_1^\bullet$ or ϱ_1° based on the positive ($\Pi^\bullet$) or negative (Π°) detection outcome of the idler mode (ϱ_2) measurement utilizing an ideal avalanche photodiode (APD).

A fragment of light from the signal mode is tapped off using a strongly unbalanced beam splitter (BS) with transmittance ζ.

(1) The signal mode of light in an arbitrary state characterized by a density operator ϱ_1 is introduced into the procedure, along the idler mode of light in a vacuum state, described by an appropriate density operator ϱ_2. The modes form a bipartite state, characterized by the density operator

$$\begin{aligned} \varrho &= \varrho_1 \otimes \varrho_2 \\ &= \varrho_1 \otimes |0\rangle_2 \langle 0| \end{aligned} \tag{II.1}$$

obtained as tensor product $\otimes$ of the individual density operators ϱ_1, ϱ_2.

(2) The signal and idler modes interact on a strongly unbalanced beam splitter with transmittance $\zeta \in (0, 1)$. The interaction is described by a Gaussian unitary operator

$$U_{12}(\vartheta) = \exp\left[-\imath\vartheta\left(a_1 a_2^\dagger + a_1^\dagger a_2\right)\right] , \tag{II.2}$$

where $\vartheta = \arccos\sqrt{\zeta}$. The density operator ϱ of the bipartite system is then transformed by the beam splitter operation $U_{12}(\vartheta)$ into

$$\varrho' = U_{12}(\vartheta)\, \varrho\, U_{12}^\dagger(\vartheta) . \tag{II.3}$$

As a result of the beam splitter interaction, the idler mode incorporates the reflected fraction of the signal mode of light.

(3) Whether the subtraction procedure is successful or not is determined by the idler mode measurement utilizing an ideal avalanche photodiode, which is completely represented by a pair of positive operator valued measure elements [14] corresponding to the positive $\Pi^{\bullet} = \mathbb{1} - |0\rangle_2 \langle 0|$ (click) and the negative $\Pi^{\circ} = |0\rangle_2 \langle 0|$ (no click) detection outcomes.

Both the probabilities $P_{\bullet}$ of a successful and $P_{\circ}$ of an unsuccessful subtraction

$$P_{\bullet} = \mathrm{Tr}\left[\varrho' \Pi^{\bullet}\right] , \quad P_{\circ} = \mathrm{Tr}\left[\varrho' \Pi^{\circ}\right] , \tag{II.4}$$

along with the respective marginal density operators

$$\varrho_1^{\bullet} = \mathrm{Tr}_2\left[\varrho' \Pi^{\bullet}\right] \left(\mathrm{Tr}\left[\varrho' \Pi^{\bullet}\right]\right)^{-1} , \quad \varrho_1^{\circ} = \mathrm{Tr}_2\left[\varrho' \Pi^{\circ}\right] \left(\mathrm{Tr}\left[\varrho' \Pi^{\circ}\right]\right)^{-1} \tag{II.5}$$

are obtained using the positive valued measure operator formalism [14].

B Inefficient detection regime

So far the detection mechanism utilized an ideal avalanche photodiode detector. In practice, however, the avalanche photodiode possesses a limited detection efficiency only and has to be taken into account in the model of the single photon subtraction procedure. Such a detector may be modeled [9, 22] using a virtual ancillary mode of light in a vacuum state, which interacts with the original idler mode on a virtual beam splitter of transmittance equal to the detection efficiency $\eta \in (0, 1)$.

The revised conceptual scheme of the procedure is presented in Figure II.2, accommodating the necessary modifications introduced by the model of an inefficient avalanche photodiode. The scheme is divided into five parts — preparation of the the signal, idler and the virtual ancillary modes (1), tapping off a fraction of the signal mode (2), interaction of the idler mode with the virtual ancillary mode in a vacuum state on te virtual beam splitter, accounting for losses due to the limited detection efficiency in (3), discarding the virtual mode (4) and finally measuring the idler mode utilizing an ideal avalanche photodiode in (5).

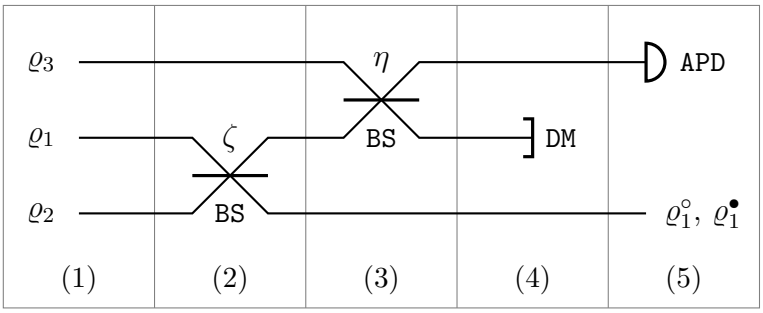

Figure II.2: The procedure transforms the initial signal mode density operator ϱ_1 into either $\varrho_1^\bullet$ or ϱ_1° based on the positive ($\Pi^\bullet$) or negative (Π°) detection outcome of the idler mode (ϱ_2) measurement utilizing an inefficient avalanche photodiode, modeled with an ideal photodiode (APD), a virtual beam splitter (BS) of transmittance η equal to the efficiency of the detector and a virtual ancillary mode (ϱ_3) in a vacuum state, which is then discarded (DM).

A fragment of light from the signal mode is tapped off using a strongly unbalanced beam splitter (BS) with transmittance ζ.

(1) In contrast with the ideal detection regime, an additional ancillary mode of light in a vacuum state is introduced into the procedure, forming a tripartite state characterized by the density operator

$$\begin{aligned} \varrho &= \varrho_1 \otimes \varrho_2 \otimes \varrho_3 \\ &= \varrho_1 \otimes |0\rangle_2 \langle 0| \otimes |0\rangle_3 \langle 0| \ . \end{aligned} \tag{II.6}$$

(2) As in the ideal detection regime, the signal and the idler mode interact on a beam splitter of transmittance $\zeta \in (0,1)$. The interaction is described by the Gaussian operator (II.2)

$$U_{12}(\vartheta) = \exp\left[-\imath\vartheta\left(a_1 a_2^\dagger + a_1^\dagger a_2\right)\right] , \tag{II.7}$$

with the parameter $\vartheta = \arccos\sqrt{\zeta}$. The tripartite density operator is then transformed by the unitary operator $U_{12}(\vartheta)$ into

$$\varrho' = U_{12}(\vartheta)\, \varrho\, U_{12}^\dagger(\vartheta) \ , \tag{II.8}$$

where the marginal density operator ϱ_3' of the virtual ancillary mode remains unchanged due to the structure of the $U_{12}(\vartheta)$ operator.

(3) The inefficient avalanche photodiode is modeled using a virtual ancillary mode of light in a vacuum state, which interacts with the idler mode on a virtual beam splitter with transmittance equal to the efficiency $\eta \in (0,1)$, accounting for the lossess caused by the limited efficiency of detection. The beam splitter interaction is described by a Gaussian unitary operator similar to (II.7)

$$U_{23}(\varkappa) = \exp\left[-\imath\varkappa\left(a_2 a_3^\dagger + a_2^\dagger a_3\right)\right] , \tag{II.9}$$

with the parameter $\varkappa = \arccos\sqrt{\eta}$. The transformed density operator ϱ'' is obtained similarly to (II.8) in the form

$$\varrho'' = U_{23}(\varkappa)\,\varrho'\,U_{23}^\dagger(\varkappa) . \tag{II.10}$$

(4) The newly introduced virtual ancillary mode accounts for the losses in the model of inefficient avalanche photodiode. It is discarded in order to actually model the loss of information contained within the mode. The state is therefore traced out of the tripartite state (II.10), yielding a marginal bipartite state characterized by the density operator

$$\varrho''' = \mathrm{Tr}_3\left[\varrho''\right] . \tag{II.11}$$

The resulting marginal state is then measured by an ideal avalanche photodiode, in the very same fashion as the bipartite state in the ideal detection regime.

(5) The detection process is the same as in the final part (3) of the ideal detection regime, with the only difference being that the marginal density operator ϱ''' is used instead of ϱ' in (II.4) and (II.5).

Both the aforementioned relations are derived for the operator ϱ''' obtained in the previous step to provide an unified picture of the transformation of the initial density operator ϱ_1 induced by the subtraction procedure, yielding the respective probabilities

$$P_\bullet = \mathrm{Tr}\left[\varrho'''\Pi^\bullet\right] = \mathrm{Tr}\left\{\mathrm{Tr}_3\left[U_{23}(\varkappa)\,U_{12}(\vartheta)\,\varrho\,U_{12}^\dagger(\vartheta)\,U_{23}^\dagger(\varkappa)\right]\Pi^\bullet\right\} , \tag{II.12}$$

$$P_\circ = \mathrm{Tr}\left[\varrho'''\Pi^\circ\right] = \mathrm{Tr}\left\{\mathrm{Tr}_3\left[U_{23}(\varkappa)\,U_{12}(\vartheta)\,\varrho\,U_{12}^\dagger(\vartheta)\,U_{23}^\dagger(\varkappa)\right]\Pi^\circ\right\} \tag{II.13}$$

and relations pertaining to the marginal density operators

$$\begin{aligned}\varrho_1^{\bullet} P_{\bullet} &= \mathrm{Tr}_2\left[\varrho'''\Pi^{\circ}\right] \\ &= \mathrm{Tr}_2\left\{\mathrm{Tr}_3\left[U_{23}\left(\varkappa\right)U_{12}\left(\vartheta\right)\varrho\, U_{12}^{\dagger}\left(\vartheta\right)U_{23}^{\dagger}\left(\varkappa\right)\right]\Pi^{\bullet}\right\},\end{aligned} \tag{II.14}$$

$$\begin{aligned}\varrho_1^{\circ} P_{\circ} &= \mathrm{Tr}_2\left[\varrho'''\Pi^{\circ}\right] \\ &= \mathrm{Tr}_2\left\{\mathrm{Tr}_3\left[U_{23}\left(\varkappa\right)U_{12}\left(\vartheta\right)\varrho\, U_{12}^{\dagger}\left(\vartheta\right)U_{23}^{\dagger}\left(\varkappa\right)\right]\Pi^{\circ}\right\},\end{aligned} \tag{II.15}$$

where $\varrho = \varrho_1 \otimes |0\rangle_{\,2}\langle 0| \otimes |0\rangle_{\,3}\langle 0|$ was defined in (II.6).

2 Phase space representation, Gaussian signal modes

The original objective of the subtraction procedure was to provide a method of creating non–Gaussian states of light. The method, along with its improved version is later in chapter IV applied to signal modes of light in a particular class of Gaussian states, i.e., squeezed vacuum states. The procedure is therefore described in the phase space representation using Wigner quasiprobability distribution functions, as these provide a rather convenient method of Gaussian state description.

A Inefficient detection regime

The description of the **inefficient detection regime**, which was done in the subsection II.1.B, is reproduced in the phase space representation. The assumption of the signal mode of light being in a squeezed vacuum state allows further evaluation and discussion of both the probability of successful (II.12) and unsuccessful (II.13) subtraction and also of the relations (II.14) and (II.15) describing the transformation of the signal mode state. The conceptual scheme presented in Figure II.3 is similarly to Figure II.2 divided into five parts.

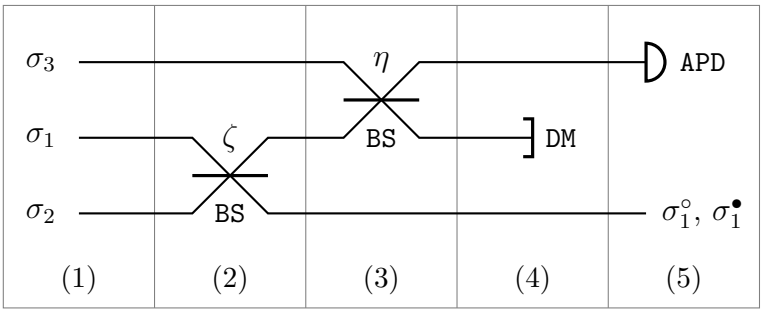

Figure II.3: The procedure transforms the initial signal mode variance matrix σ_1 into either $\sigma_1^\bullet$ or σ_1° based on the positive ($W_{\Pi\bullet}$) or negative ($W_{\Pi\circ}$) detection outcome of the idler mode (σ_2) measurement utilizing an inefficient avalanche photodiode, modeled with an ideal photodiode (APD), a virtual beam splitter (BS) of transmittance η equal to the efficiency of the detector and a virtual ancillary mode in a vacuum state (σ_3), which is then discarded (DM).

A fragment of light from the signal mode is tapped off using a strongly unbalanced beam splitter (BS) with transmittance ζ.

(1) The signal mode of light is prepared in a Gaussian state characterized by a diagonal variance matrix $\sigma_1 = \mathrm{diag}\,(\nu_1, \nu_2)$ and a zero vector of mean values μ_1. Both the idler and the virtual ancillary mode are found in vacuum states characterized by their respective variance matrices $\sigma_2 = \sigma_3 = 2^{-1}\mathbb{I}$ and zero vectors of mean values μ_2, μ_3.

The tripartite system is characterized by a diagonal 6×6 variance matrix

$$\begin{aligned} \sigma &= \sigma_1 \oplus \sigma_2 \oplus \sigma_3 \\ &= \sigma_1 \oplus 2^{-1}\mathbb{I} \oplus 2^{-1}\mathbb{I}\,, \end{aligned} \tag{II.16}$$

which is obtained in the form of a direct sum $\oplus$ of the individual variance matrices σ_1, σ_2 and σ_3. The corresponding Wigner function W_ϱ of the system generally characterized by the density operator ϱ derived in (II.6) is readily obtained either by directly multiplying the individual Wigner functions

$$W_\varrho\,(x_1, p_1, x_2, p_2, x_3, p_3) = W_1\,(x_1, p_1)\, W_2\,(x_2, p_2)\, W_3\,(x_3, p_3) \tag{II.17}$$

or by constructing the respective Gaussian Wigner function from the previ-

ously derived variance matrix σ

$$W_\varrho\left(x_1, p_1, x_2, p_2, x_3, p_3\right) = G\left(\xi, \sigma\right) , \tag{II.18}$$

where the vector $\xi = (x_1, p_1, x_2, p_2, x_3, p_3)^\intercal$ comprises the respective phase space quadrature variables.

(2) Following that the beam splitter interaction is a Gaussian operation characterized by unitary operators like (II.2) or (II.7), the transformed tripartite state (II.8) remains Gaussian. The unitary operator (II.7) is in the phase space representation characterized by the linear transformation of the variance matrix (II.16)

$$\sigma' = \left[V\left(\zeta\right) \oplus \mathbb{I}\right] \sigma \left[V\left(\zeta\right) \oplus \mathbb{I}\right]^\intercal \tag{II.19}$$

with the matrix $V\left(\zeta\right)$ defining the linear transformation of an arbitrary beam splitter operation in the form of

$$V\left(\zeta\right) = \begin{pmatrix} \sqrt{\zeta} & 0 & \sqrt{1-\zeta} & 0 \\ 0 & \sqrt{\zeta} & 0 & \sqrt{1-\zeta} \\ \sqrt{1-\zeta} & 0 & \sqrt{\zeta} & 0 \\ 0 & \sqrt{1-\zeta} & 0 & \sqrt{\zeta} \end{pmatrix} . \tag{II.20}$$

(3) The inefficient avalanche photodiode is modeled using a virtual beam splitter and a virtual ancillary mode in a vacuum state. The interaction of the virtual and idler modes on the virtual beam splitter was described by the unitary operator (II.9) in the previous section.

Similarly to the recently derived linear transformation (II.19), the variance matrix σ' is transformed into

$$\sigma'' = \left[\mathbb{I} \oplus V\left(\eta\right)\right] \sigma' \left[\mathbb{I} \oplus V\left(\eta\right)\right]^\intercal \tag{II.21}$$

by the virtual beam splitter, where the transformation matrix $V\left(\eta\right)$ takes the form of (II.20).

(4) The second ancillary mode used in the inefficient photodiode model is discarded — it is traced out of the tripartite state characterized by the variance

matrix σ''. The marginal bipartite state is obtained with the aid of the Wigner's overlap formula (I.10) in the integral form

$$\begin{aligned} W_{\varrho'''}(\xi') &= \int\limits_{-\infty}^{+\infty}\int\limits_{-\infty}^{+\infty} W_{\varrho''}(\xi)\,\mathrm{d}\xi_3 \\ &= \int\limits_{-\infty}^{+\infty}\int\limits_{-\infty}^{+\infty} G(\xi,\sigma'')\,\mathrm{d}\xi_3\,, \end{aligned} \tag{II.22}$$

where the vector $\xi' = (x_1, p_1, x_2, p_2)^\intercal$ comprises the remaining phase space quadrature variables and the vector $\xi_3 = (x_3, p_3)^\intercal$ covers the quadrature variables related to the virtual ancillary mode.

Following the integrand $G(\xi, \sigma'')$ is a Gaussian function, the integration in (II.22) results in a Gaussian Wigner function

$$W_{\varrho'''}(\xi') = G(\xi', \sigma''') \tag{II.23}$$

characterized by the no longer diagonal 4×4 variance matrix

$$\sigma''' = Y(\eta)\, V(\zeta)\, [\sigma_1 \oplus \sigma_2]\, V^\intercal(\zeta)\, Y^\intercal(\eta) + 2^{-1}\big[\mathbb{I} - Y^2(\eta)\big]\big[\mathbb{O} \oplus \mathbb{I}\big]\,, \tag{II.24}$$

where $Y(\eta) = \mathbb{I} \oplus \sqrt{\eta}\,\mathbb{I}$. The variance matrix σ''' is essentially the matrix σ'' stripped off of the rows and columns pertaining to the virtual ancillary mode.

(5) As the relations (II.4) and (II.5) suggest, an ideal avalanche detector is characterized by a pair of distinct outcome events represented by positive operator value measure elements Π° and $\Pi^\bullet$ with respective Wigner functions

$$W_{\Pi^\circ}(\xi_2') = G\left(\xi_2', 2^{-1}\mathbb{I}\right)\,, \quad W_{\Pi^\bullet}(\xi_2') = (2\pi)^{-1} - G\left(\xi_2', 2^{-1}\mathbb{I}\right)\,, \tag{II.25}$$

where $\xi_2' = (x_2, p_2)^\intercal$. The first function ($W_{\Pi^\circ}$) represents the negative detection outcome (no–click), i.e., the **unsuccessful** execution of the procedure as no photons are subtracted from the signal state, while the other one ($W_{\Pi^\bullet}$) describes the positive detection event (click), i.e., the **successful** subtraction of at least a single photon.

Both the outcome probability $P_\circ$ and the marginal Wigner function $W_1^\circ(\xi_1')$

associated with the **unsuccessful** subtraction are obtained using the Wigner's overlap formula (I.10) from (II.13) and (II.15) with the help of (II.25)

$$\begin{aligned} P_{\circ} &= 2\,\pi \int\limits_{-\infty}^{+\infty} \int\limits_{-\infty}^{+\infty} W_{\varrho'''}\left(\xi'\right) W_{\Pi^{\circ}}\left(\xi'\right)\,\mathrm{d}\xi' \\ &= 2\,\pi \int\limits_{-\infty}^{+\infty} \int\limits_{-\infty}^{+\infty} G\left(\xi', \sigma'''\right) G\left(\xi_2', 2^{-1}\mathbb{I}\right)\,\mathrm{d}\xi'\,, \end{aligned} \tag{II.26}$$

$$\begin{aligned} W_1^{\circ}\left(\xi_1'\right) P_{\circ} &= 2\,\pi \int\limits_{-\infty}^{+\infty} \int\limits_{-\infty}^{+\infty} W_{\varrho'''}\left(\xi'\right) W_{\Pi^{\circ}}\left(\xi'\right)\,\mathrm{d}\xi_2' \\ &= 2\,\pi \int\limits_{-\infty}^{+\infty} \int\limits_{-\infty}^{+\infty} G\left(\xi', \sigma'''\right) G\left(\xi_2', 2^{-1}\mathbb{I}\right)\,\mathrm{d}\xi_2'\,, \end{aligned} \tag{II.27}$$

where $\xi_1' = (x_1, p_1)$ and $\xi_2' = (x_2, p_2)$. Following that the composite integrand in (II.27) is a Gaussian function, the marginal Wigner function $W_1^{\circ}\left(\xi_1'\right)$ is Gaussian as well.

The probability $P_{\bullet}$ and the marginal Wigner function $W_1^{\bullet}\left(\xi_1'\right)$ associated with the **successful** subtraction are obtained similarly from (II.12) and (II.14)

$$\begin{aligned} P_{\bullet} &= 2\,\pi \int\limits_{-\infty}^{+\infty} \int\limits_{-\infty}^{+\infty} W_{\varrho'''}\left(\xi'\right) W_{\Pi^{\bullet}}\left(\xi'\right)\,\mathrm{d}\xi' \\ &= 2\,\pi \int\limits_{-\infty}^{+\infty} \int\limits_{-\infty}^{+\infty} G\left(\xi', \sigma'''\right) \left[(2\,\pi)^{-1} - G\left(\xi_2', 2^{-1}\mathbb{I}\right)\right]\,\mathrm{d}\xi' \\ &= \int\limits_{-\infty}^{+\infty} \int\limits_{-\infty}^{+\infty} G\left(\xi', \sigma'''\right)\,\mathrm{d}\xi' - 2\,\pi \int\limits_{-\infty}^{+\infty} \int\limits_{-\infty}^{+\infty} G\left(\xi', \sigma'''\right) G\left(\xi_2', 2^{-1}\mathbb{I}\right)\,\mathrm{d}\xi' \\ &= 1 - P_{\circ}\,, \end{aligned} \tag{II.28}$$

$$
\begin{aligned}
W_1^{\bullet}\left(\xi_1'\right) P_{\bullet} &= 2\,\pi \int_{-\infty}^{+\infty}\int_{-\infty}^{+\infty} W_{\varrho'''}\left(\xi'\right) W_{\Pi\bullet}\left(\xi'\right)\,\mathrm{d}\xi_2' \\
&= 2\,\pi \int_{-\infty}^{+\infty}\int_{-\infty}^{+\infty} G\left(\xi', \sigma'''\right)\left[\left(2\,\pi\right)^{-1} - G\left(\xi_2', 2^{-1}\mathbb{I}\right)\right]\,\mathrm{d}\xi_2' \qquad \text{(II.29)} \\
&= \int_{-\infty}^{+\infty} G\left(\xi', \sigma'''\right)\,\mathrm{d}\xi_2' - W_1^{\circ}\left(\xi_1'\right) P_{\circ}\,,
\end{aligned}
$$

where the marginal Wigner function $W_1^{\bullet}\left(\xi_1'\right)$ is no longer Gaussian, as it is a linear combination of two Gaussian functions.

B Negative detection outcome

The Gaussian Wigner function (II.27) of the unsuccessfully subtracted state is characterized by a diagonal variance matrix σ_1°. Notably the relation between σ_1° and the initial variance matrix $\sigma_1 = \mathrm{diag}\left(\nu_1, \nu_2\right)$ of the signal mode is found to be

$$
\sigma_1^{\circ} = \mathrm{diag}\left(\Xi\left(\nu_1\right), \Xi\left(\nu_2\right)\right)\,, \qquad \text{(II.30)}
$$

where the function $\Xi\left(\nu\right)$ defines the transformation of each diagonal element ν_1, ν_2

$$
\Xi\left(\nu\right) = \frac{1}{2} + \frac{\zeta\left(2\nu - 1\right)}{2 + \eta\left(1 - \zeta\right)\left(2\nu - 1\right)}\,, \qquad \text{(II.31)}
$$

while the probability relation (II.26) of unsuccessful subtraction is found to be

$$
P_{\circ}\left(\sigma_1\right) = \frac{2}{\sqrt{\det\left[2\mathbb{I} + \eta\left(1 - \zeta\right)\left(2\sigma_1 - \mathbb{1}\right)\right]}} \qquad \text{(II.32)}
$$

with the argument σ_1 emphasizing the dependence of the probability on the variance of the signal mode. Moreover the Gaussian Wigner function (II.27) may be expressed as

$$
W_1^{\circ}\left(\xi_1'\right) = G\left(\xi_1', \sigma_1^{\circ}\right) \qquad \text{(II.33)}
$$

with the knowledge of the recently derived variance matrix σ_1° of the unsuccessfully subtracted state.

C Positive detection outcome, successful subtraction of a single photon

The non–Gaussian Wigner function (II.29) of the unsuccessfully subtracted state can not be described by a single variance matrix; the normalized Wigner function is a weighed linear combination

$$W_1^{\bullet}\left(\xi_1'\right) = \frac{1}{P_{\bullet}(\sigma_1)}\left[G\left(\xi_1', \frac{\mathbb{I}+\zeta(2\sigma_1-\mathbb{I})}{2}\right) - G(\xi_1', \sigma_1')P_{\circ}(\sigma_1)\right] , \tag{II.34}$$

which depends on the variance matrix σ_1 of the signal mode, the Gaussian Wigner function $W_1^{\circ}(\xi_1') = G\left(\xi_1', \sigma_1^{\circ}\right)$ of the unsuccessfully subtracted state and both the probabilities of successful and unsuccessful detection probability. The former probability $P_{\bullet}\left(\sigma_1\right)$ is readily obtained in the relation (II.28) as

$$P_{\bullet}\left(\sigma_1\right) = 1 - P_{\circ}\left(\sigma_1\right) . \tag{II.35}$$

Formally the $W_1^{\bullet}(\xi_1')$ derived in (II.34) is a function of the vector $\xi_1' = (x_1, p_1)$, the variance matrix σ_1 and the matrix σ_1° readily obtained in (II.30).

Chapter III

Iterative single photon subtraction procedure

An improved version of the single step single photon subtraction procedure is introduced in this chapter with the intention of enhancing the probability of a successful subtraction of a single photon.

The most significant difference between the original and the improved procedure lies in the manner in which the unsuccessful subtraction is handled: in contrast to the original version, the unsuccessfully subtracted states are iteratively recycled until the procedure either finally succeeds or a reasonable number of attempts (iterations) is exceeded. This can be achieved, for example, by employing an optical resonator equipped with a shutter [23]. Following the nature of the modification, the proposed procedure is called **iterative single photon subtraction procedure**.

1 Breakdown of the iterative procedure model

The iterative subtraction is realized with a number of individual single step procedures concatenated together; the conceptual scheme of the iterative procedure presented in Figure III.1 is divided into three parts, each describing a different stage of the iterative process, i.e., the preparation of the initial signal mode (1), attempting the subtraction without any success (2) and eventually succeeding at

it in (3).

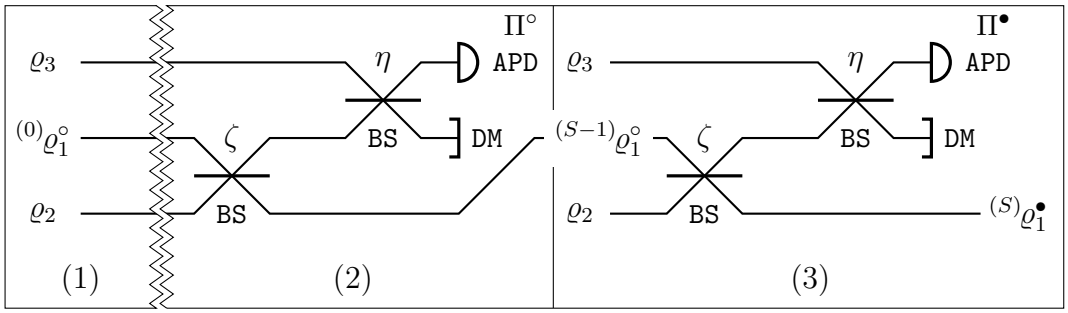

Figure III.1: The iterative procedure eventually transforms the initial signal mode density operator $^{(0)}\varrho_1^\circ$ prepared in the part (1) into $^{(S)}\varrho_1^\bullet$ in the iteration step (S). The part (2) represents the preceding $(S-1)$ unsuccessful attempts at subtraction, until at least a single photon is successfully subtracted in the part (3).

The conceptual scheme comprises several concatenated single step procedures, which were described in detail in the subsection II.1.B. The symbol `APD` denotes an ideal avalanche photodiode, `BS` a beam splitter and finally `DM` a mode discarder.

(1) The initial signal mode of light is prepared in an arbitrary state characterized by the density operator $^{(0)}\varrho_1^\circ$ similarly to the part (1) of the inefficient detection regime introduced in the subsection II.1.B.

The upper left index (S) in $^{(S)}\varrho_1^\circ$ denotes the iteration step (S) in which the the density operator of the signal mode was produced: the initial density operator $^{(0)}\varrho_1^\circ$ is henceforth denoted by the (0) upper left index.

(2) The iterative subtraction procedure has not yet successfully subtracted any photon from the signal mode of light in this stage. The probability of an unsuccessful subtraction of a single photon from the signal mode of light in a state characterized by the density operator $^{(S-1)}\varrho_1^\circ$ is derived by adopting the relation (II.13).

However, the probability $P_\circ\left(^{(S-1)}\varrho_1^\circ\right)$ in question only provides an incomplete picture of the situation, as it fails to account for the conditional probability of the procedure not succeeding in the previous steps of the iteration. The conditional probability

$$^{(S)}P_\circ = \prod_{Z=1}^{S} P_\circ\left(^{(Z-1)}\varrho_1^\circ\right) \tag{III.1}$$

therefore yields a complete probability of an unsuccessful single photon subtraction in the iteration step (S) of the iterative procedure. The first term of the product in (III.1) is assumed to satisfy the condition $P_{\circ}\left({}^{(0)}\varrho_1^{\circ}\right) = 1$.

The density operator ${}^{(S-1)}\varrho_1^{\circ}$ is in each subsequent unsuccessful iteration step (S) transformed according to the relation (II.15) into ${}^{(S)}\varrho_1^{\circ}$ with the symbols ϱ_1 and ϱ_1° taken to be

$$\varrho_1 \to {}^{(S-1)}\varrho_1^{\circ}\,, \quad \varrho_1^{\circ} \to {}^{(S)}\varrho_1^{\circ}\,. \tag{III.2}$$

(3) The iterative subtraction procedure eventually succeeds at subtracting at least a single photon from the signal mode in the final iteration step (S). The probability of a successful subtraction from the state characterized by the respective density operator ${}^{(S-1)}\varrho_1^{\circ}$ is obtained by adopting (II.12). The conditional probability is derived in the product form

$${}^{(S)}P_{\bullet} = P_{\bullet}\left({}^{(S-1)}\varrho_1^{\circ}\right) {}^{(S-1)}P_{\circ} \tag{III.3}$$

of the conditional probability ${}^{(S)}P_{\circ}$ of an unsuccessful subtraction in previous iteration steps and the probability $P_{\bullet}$ of a successful subtraction in the current step. The relation can be further simplified into the form

$$\begin{aligned} {}^{(S)}P_{\bullet} &= P_{\bullet}\left({}^{(S-1)}\varrho_1^{\circ}\right) {}^{(S-1)}P_{\circ} \\ &= \left[1 - P_{\circ}\left({}^{(S-1)}\varrho_1^{\circ}\right)\right] \prod_{Z=1}^{S-1} P_{\circ}\left({}^{(Z-1)}\varrho_1^{\circ}\right) \\ &= \prod_{Z=1}^{S-1} P_{\circ}\left({}^{(Z-1)}\varrho_1^{\circ}\right) - \prod_{Z=1}^{S} P_{\circ}\left({}^{(Z-1)}\varrho_1^{\circ}\right) \\ &= {}^{(S-1)}P_{\circ} - {}^{(S)}P_{\circ}\,, \end{aligned} \tag{III.4}$$

which turns out to be quite handy in the following paragraph. The respective density operator ${}^{(S)}\varrho_1^{\bullet}$ of the successfully subtracted state is obtained by employing the transformation (II.14), where the symbols ϱ_1 and $\varrho_1^{\bullet}$ are substituted according to the

$$\varrho_1 \to {}^{(S-1)}\varrho_1^{\circ}\,, \quad \varrho_1^{\bullet} \to {}^{(S)}\varrho_1^{\bullet}\,. \tag{III.5}$$

The iterative single photon subtraction procedure was introduced as a clearly probabilistic process; following its probabilistic nature it is only sensible to describe the procedure using the resulting density operator $\varrho_1^{(S)}$ of the successfully subtracted state in in up to S iteration steps. The overall probability $Q^{(S)}$ of a successful subtraction of at least a single photon in up to S iteration steps is then derived as a sum

$$Q^{(S)} = \sum_{Z=1}^{S} {}^{(Z)}P_{\bullet} \tag{III.6}$$

of respective conditional probabilities ${}^{(Z)}P_{\bullet}$ of successful subtraction in individual iteration steps. It is possible to further simplify the expression with the aid of the expanded relation (III.4) into the form

$$\begin{aligned} Q^{(S)} &= \sum_{Z=1}^{S} {}^{(Z)}P_{\bullet} = \sum_{Z=1}^{S} {}^{(Z-1)}P_{\circ} - {}^{(Z)}P_{\circ} \\ &= {}^{(0)}P_{\circ} - {}^{(1)}P_{\circ} + {}^{(1)}P_{\circ} - {}^{(2)}P_{\circ} + \cdots - {}^{(S-1)}P_{\circ} + {}^{(S-1)}P_{\circ} - {}^{(S)}P_{\circ} \\ &= 1 - {}^{(S)}P_{\circ}\,, \end{aligned} \tag{III.7}$$

which implies that the expression $Q^{(S)}$ yields a valid probability, as the condition $0 \leq Q^{(S)} \leq 1$ clearly holds. The resulting density operator characterizing the successfully subtracted state in up to S iteration steps is obtained in the form of a statistical mixture of individual density operators

$$\varrho_1^{(S)} = \frac{1}{Q^{(S)}} \sum_{Z=1}^{S} {}^{(Z)}P_{\bullet}\, {}^{(Z)}\varrho_1^{\bullet}\,. \tag{III.8}$$

2 Phase space representation, Gaussian signal modes

Similarly to the section II.2, the iterative single photon subtraction procedure is described in the phase space representation as well. The signal mode is assumed to be in a Gaussian state completely characterized by a diagonal variance matrix, allowing a further evaluation of the relations obtained in the section III.1. The conceptual scheme presented in the , is similarly to Figure III.1 divided into three parts.

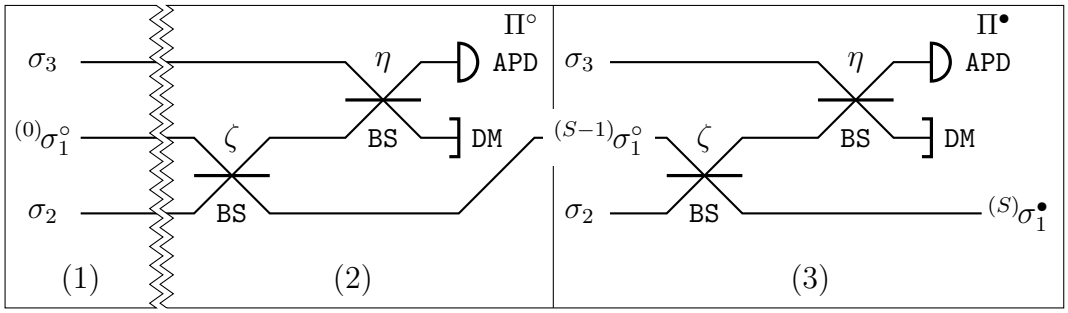

Figure III.2: The iterative procedure eventually transforms the initial signal mode density operator ${}^{(0)}\sigma_1^\circ$ prepared in the part (1) into ${}^{(S)}\sigma_1^\bullet$ in the iteration step (S). The part (2) represents the preceding $(S-1)$ unsuccessful attempts at subtraction, until at least a single photon is successfully subtracted in the part (3).

The conceptual scheme comprises several concatenated single step procedures, which were described in detail in the subsection II.2.A. The symbol `APD` denotes an ideal avalanche photodiode, `BS` a beam splitter and finally `DM` a mode discarder.

(1) The initial signal mode of light is prepared in a Gaussian state characterized by a diagonal variance matrix

$$ {}^{(0)}\sigma_1 = \mathrm{diag}\left({}^{(0)}\nu_1, {}^{(0)}\nu_2\right) \tag{III.9} $$

and a zero vector of mean values ${}^{(0)}\mu_1 = 0$. Notably, the condition ${}^{(S)}\mu_1 = 0$ holds for each iteration step (S) .

(2) The variance matrix ${}^{(S)}\sigma_1 = \mathrm{diag}\left({}^{(S)}\nu_1, {}^{(S)}\nu_2\right)$ is according to (II.30) transformed with each subsequent unsuccessful iteration step. The relation (II.30) yields a recurrently defined sequence

$$ {}^{(S+1)}\sigma_1 = \mathrm{diag}\left(\Xi\left({}^{(S)}\nu_1\right), \Xi\left({}^{(S)}\nu_2\right)\right), \tag{III.10} $$

which characterizes the evolution of the variance matrix in the course of the iterative procedure. The recurrently defined sequence can be conveniently expressed in the positional form

$$ {}^{(S)}\nu = \frac{1}{2} + \frac{\zeta^S\left(2\,{}^{(0)}\nu - 1\right)}{2 + \eta\left(1-\zeta^S\right)\left(2\,{}^{(0)}\nu - 1\right)}, \tag{III.11} $$

where ${}^{(S)}\nu$ stands for both the diagonal elements ${}^{(S)}\nu_1$ and ${}^{(S)}\nu_2$ of the ${}^{(S)}\sigma_1$.

The sequence (III.11) depends solely on the pair of parameters ζ, η and the initial variance matrix ${}^{(0)}\sigma_1 = \mathrm{diag}\left({}^{(0)}\nu_1, {}^{(0)}\nu_2\right)$.

The probability of an unsuccessful subtraction of a single photon from the signal mode of light in a state characterized by the variance matrix ${}^{(S-1)}\sigma_1$ in the iteration step (S) is obtained by adopting the familiar equation (II.32). The conditional probability ${}^{(S)}P_\circ$ introduced earlier in (III.1) is derived here as a product

$$ {}^{(S)}P_\circ = \prod_{Z=1}^{S} P_\circ\left({}^{(Z-1)}\sigma_1\right) \tag{III.12} $$

of individual probabilities $P_\circ\left({}^{(Z)}\sigma_1\right)$ from (II.32).

(3) The probability of a successful subtraction in the iteration step (S) is obtained (II.35). Similarly to (III.4) the conditional probability ${}^{(S)}P_\bullet$ is derived in the form of

$$ {}^{(S)}P_\bullet = P_\bullet\left({}^{(S-1)}\sigma_1^\circ\right) {}^{(S-1)}P_\circ = {}^{(S-1)}P_\circ - {}^{(S)}P_\circ\,. \tag{III.13} $$

It was established in the section II.2 that the successfully subtracted mode of light is no longer in a Gaussian state; its respective Wigner function is obtained in (II.34) as a linear combination of a pair of Gaussian Wigner functions. The adopted version of (II.34) in the iterative procedure constitutes

$$ \begin{aligned} {}^{(S)}W_1^\bullet(\xi_1') = {} & \frac{1}{P_\bullet({}^{(S-1)}\sigma_1^\circ)}\, G\left(\xi_1', \frac{\mathbb{I} + \zeta(2\,{}^{(S-1)}\sigma_1^\circ - \mathbb{I})}{2}\right) - \\ & \frac{1}{P_\bullet({}^{(S-1)}\sigma_1^\circ)}\, G(\xi_1', {}^{(S)}\sigma_1^\circ) P_\circ({}^{(S-1)}\sigma_1^\circ)\,. \end{aligned} \tag{III.14} $$

In the preceding section the iterative single photon subtraction procedure was characterized by a pair of equations (III.7) and (III.8), which gave a general description of effects of the subtraction procedure on fields of light in arbitrary states. In this section, the vast amount of possible quantum states of light was limited to the class of squeezed vacuum states; with this assumption the procedure was described in the phase space representation, using the Wigner distribution functions in particular.

Similarly to the section II.2, the constriction imposed on the class of discussed states of light grants a possibility of further evaluation of the relations describing

the effects of the procedure. The overall probability $Q^{(S)}$ of successful subtraction in up to S iteration steps

$$Q^{(S)} = 1 - {}^{(S)}P_{\circ} \tag{III.15}$$

is obtained similarly to (III.7), with the only difference arising from the formulation of the probability ${}^{(S)}P_{\circ}$ in (III.13). The successfully subtracted state is characterized by a Wigner function obtained as a weighed linear combination of Wigner functions pertaining to individual iteration steps

$$W_1^{(S)}\left(\xi_1'\right) = \frac{1}{Q^{(S)}} \sum_{Z=1}^{S} {}^{(Z)}P_{\bullet}\, {}^{(Z)}W_1^{\bullet}\left(\xi_1'\right) , \tag{III.16}$$

which may be expanded using (III.14) and (III.13) into

$$\begin{aligned} W_1^{(S)}\left(\xi_1'\right) = \frac{1}{Q^{(S)}} \sum_{Z=1}^{S} G\left(\xi_1', \frac{\mathbb{I} + \zeta(2\,{}^{(Z-1)}\sigma_1^{\circ} - \mathbb{I})}{2}\right) {}^{(Z-1)}P_{\circ} - \\ G(\xi_1', {}^{(Z)}\sigma_1^{\circ})\,{}^{(Z)}P_{\circ}\,. \end{aligned} \tag{III.17}$$

The introduction of the iterative subtraction procedure would be woefully incomplete without a proper analysis of certain mathematical properties of the relations (III.15) and (III.16), namely the (uniform) convergence.

A Probability of a successful subtraction

In order to show that the sequence $Q^{(S)}$ defined in (III.15) is indeed convergent, it is imperative to investigate the conditional probability ${}^{(S)}P_{\circ}$ of unsuccessful subtraction first. The conditional probability was derived in (III.12) as a product

$${}^{(S)}P_{\circ} = \prod_{Z=1}^{S} P_{\circ}\left({}^{(Z-1)}\sigma_1^{\circ}\right) = \prod_{Z=0}^{S-1} P_{\circ}\left({}^{(Z)}\sigma_1^{\circ}\right) \tag{III.18}$$

of individual probabilities $P_{\circ}\left({}^{(Z)}\sigma_1^{\circ}\right)$. The respective diagonal variance matrices ${}^{(Z)}\sigma_1^{\circ} = \mathrm{diag}\left({}^{(Z)}\nu_1, {}^{(Z)}\nu_2\right)$ are easily determined using (III.11), which is rewritten into the form

$${}^{(S)}\nu = \frac{1}{2} + \frac{\zeta^S \chi}{2 + \eta\,(1 - \zeta^S)\,\chi} \tag{III.19}$$

using the substitution $\chi \coloneqq \left(2\,{}^{(0)}\nu - 1\right)$, where the symbol ν refers to both the diagonal elements of ${}^{(0)}\sigma_1^\circ = \mathrm{diag}\left({}^{(0)}\nu_1, {}^{(0)}\nu_2\right)$. It is highly advantageous to expand the matrix determinant in the relation (II.32) into

$$\begin{aligned} P_\circ\left({}^{(Z)}\sigma_1^\circ\right) &= \frac{2}{\sqrt{\det\left[2\mathbb{I} + \eta\,(1-\zeta)\,(2\,{}^{(Z)}\sigma_1^\circ - \mathbb{I})\right]}} \\ &= \frac{2}{\sqrt{2 + \eta\,(1-\zeta)\,(2\,{}^{(Z)}\nu_1 - 1)}\sqrt{2 + \eta\,(1-\zeta)\,(2\,{}^{(Z)}\nu_2 - 1)}} \\ &= \frac{2}{\sqrt{\alpha_Z}\sqrt{\beta_Z}}\,, \end{aligned} \tag{III.20}$$

while introducing another pair of substitutions

$$\begin{aligned} \alpha_Z &\coloneqq 2 + \eta\,(1-\zeta)\left(2\,{}^{(Z)}\nu_1 - 1\right) = 2 + \eta\,(1-\zeta)\,\frac{\zeta^Z\chi_1}{2 + \eta\,(1-\zeta^Z)\,\chi_1}\,, \\ \beta_Z &\coloneqq 2 + \eta\,(1-\zeta)\left(2\,{}^{(Z)}\nu_2 - 1\right) = 2 + \eta\,(1-\zeta)\,\frac{\zeta^Z\chi_2}{2 + \eta\,(1-\zeta^Z)\,\chi_2}\,, \end{aligned} \tag{III.21}$$

where the relation (III.19) was used. The substitutions α_Z and β_Z can be further simplified into the form

$$\begin{aligned} \alpha_Z &= 2\,\frac{2 + \eta\left(1-\zeta^{Z+1}\right)\chi_1}{2 + \eta\,(1-\zeta^Z)\,\chi_1} = 2\,\frac{u_{Z+1}}{u_Z}\,, \\ \beta_Z &= 2\,\frac{2 + \eta\left(1-\zeta^{Z+1}\right)\chi_2}{2 + \eta\,(1-\zeta^Z)\,\chi_2} = 2\,\frac{v_{Z+1}}{v_Z}\,, \end{aligned} \tag{III.22}$$

with both the α_Z and β_Z expressed as fractions of consecutive elements of structurally identical sequences

$$u_Z = 2 + \eta\left(1-\zeta^Z\right)\chi_1\,, \quad v_Z = 2 + \eta\left(1-\zeta^Z\right)\chi_2\,. \tag{III.23}$$

The relation (III.18) is rewritten using the substitution (III.20) of the $P_\circ\left({}^{(Z)}\sigma_1^\circ\right)$

$${}^{(S)}P_\circ = 2^S\prod_{Z=0}^{S-1}\frac{1}{\sqrt{\alpha_Z}\sqrt{\beta_Z}} = 2^S\sqrt{\left(\prod_{Z=0}^{S-1}\alpha_Z\right)^{-1}\left(\prod_{Z=0}^{S-1}\beta_Z\right)^{-1}}\,, \tag{III.24}$$

which can be further simplified by employing the substitution (III.22)

$$\begin{aligned}\prod_{Z=0}^{S-1}\alpha_Z &= 2^S\frac{u_1\cdots u_S}{u_0\cdots u_{S-1}} = 2^S\frac{u_S}{u_0} &&= 2^{S-1}\left[2+\eta\left(1-\zeta^S\right)\chi_1\right]\,,\\ \prod_{Z=0}^{S-1}\beta_Z &= 2^S\frac{v_1\cdots v_S}{v_0\cdots v_{S-1}} = 2^S\frac{v_S}{v_0} &&= 2^{S-1}\left[2+\eta\left(1-\zeta^S\right)\chi_2\right]\,.\end{aligned} \tag{III.25}$$

Following the previous simplification, the conditional probability ${}^{(S)}P_\circ$ is obtained in the form

$$\begin{aligned}{}^{(S)}P_\circ &= 2^S\frac{1}{\sqrt{2^{S-1}\left(2+\eta\left(1-\zeta^S\right)\chi_1\right)}\sqrt{2^{S-1}\left(2+\eta\left(1-\zeta^S\right)\chi_2\right)}}\\ &= \frac{2}{\sqrt{\left(2+\eta\left(1-\zeta^S\right)\left(2\,{}^{(0)}\nu_1-1\right)\right)}\sqrt{\left(2+\eta\left(1-\zeta^S\right)\left(2\,{}^{(0)}\nu_2-1\right)\right)}}\,,\end{aligned} \tag{III.26}$$

which can be expressed in the compact form using a matrix determinant

$${}^{(S)}P_\circ = \frac{2}{\sqrt{\det\left[2\mathbb{I}+\eta\left(1-\zeta^S\right)\left(2\,{}^{(0)}\sigma_1^\circ-\mathbb{I}\right)\right]}}\,, \tag{III.27}$$

giving the final form to the probability (III.15) of successful subtraction of a single photon in up to S iteraton steps

$$\begin{aligned}Q^{(S)} &= 1-{}^{(S)}P_\circ\\ &= 1-\frac{2}{\sqrt{\det\left[2\mathbb{I}+\eta\left(1-\zeta^S\right)\left(2\,{}^{(0)}\sigma_1^\circ-\mathbb{I}\right)\right]}}\,.\end{aligned} \tag{III.28}$$

The knowledge of (III.27) grants an insight into the convergence of the overall probability $Q^{(S)}$ by simply evaluating the limit

$$\begin{aligned}\lim_{S\to\infty}Q^{(S)} &= 1-\lim_{S\to\infty}{}^{(S)}P_\circ\\ &= 1-\lim_{S\to\infty}\frac{2}{\sqrt{\det\left[2\mathbb{I}+\eta\left(1-\zeta^S\right)\left(2\,{}^{(0)}\sigma_1^\circ-\mathbb{I}\right)\right]}}\\ &= 1-\frac{2}{\sqrt{\det\left[2\mathbb{I}+\eta\left(2\,{}^{(0)}\sigma_1^\circ-\mathbb{I}\right)\right]}}\,,\end{aligned} \tag{III.29}$$

where $\zeta \in (0,1) \implies \lim_{S\to\infty} \zeta^S = 0$. The overall probability $Q^{(S)}$ of successful subtraction of a single photon from a mode of light in an arbitrary Gaussian state in up to S iteration steps is therefore convergent. □

The value of the $Q^{(S)}$ limit corresponds to a scenario in which the transmittance of the beam splitter used to realize the subtraction is taken to be $\zeta = 0$ and the entire the signal mode is therefore reflected into the inefficient avalanche photodiode in the first step of the iteration. The limit matches the probability associated with the detection outcome $\Pi^{\bullet}$ in the direct measurement of the initial signal mode,

$$\begin{aligned} \lim_{S\to\infty} Q^{(S)} &= \lim_{\zeta\to 0} P_{\circ}\left({}^{(0)}\sigma_1^{\circ}\right) \\ &= 1 - \lim_{\zeta\to 0} \frac{2}{\sqrt{\det\left[2\mathbb{I} + \eta\,(1-\zeta)\,(2\,{}^{(0)}\sigma_1^{\circ} - \mathbb{1})\right]}} \\ &= 1 - \frac{2}{\sqrt{\det\left[2\mathbb{I} + \eta\,(2\,{}^{(0)}\sigma_1^{\circ} - \mathbb{1})\right]}}\,. \end{aligned} \tag{III.30}$$

B Wigner function of the successfully subtracted state

The uniform convergence of the series $W_1^{(S)}(\xi_1')$ defined in (III.16) is verified with the aid of the Weierstrass M–test [24]. Each summand of the function series

$$W_1^{(S)}(\xi_1') = \frac{1}{Q^{(S)}} \sum_{Z=1}^{S} {}^{(Z)}P_{\bullet}\,{}^{(Z)}W_1^{\bullet}(\xi_1') \tag{III.31}$$

is shown to be dominated by the respective conditional probability ${}^{(Z)}P_{\bullet}$ in the chain of inequalities

$${}^{(Z)}W_1^{\bullet}(\xi_1')\;{}^{(Z)}P_{\bullet} \leq |{}^{(Z)}W_1^{\bullet}(\xi_1')|\;{}^{(Z)}P_{\bullet} \leq \pi^{-1}\;{}^{(Z)}P_{\bullet} \leq {}^{(Z)}P_{\bullet}\,, \tag{III.32}$$

as every normalized real Wigner function is fundamentally bound to $|{}^{(S)}W_{\bullet}| \leq \pi^{-1}$. In order to satisfy the Weierstrass M–test, the dominating number sequence must converge as series, which it does following that the sequence $Q^{(S)}$ was originally

defined in (III.7) in the form of a number series

$$Q^{(S)} = \sum_{Z=1}^{S} {}^{(Z)}P_{\bullet}\,, \tag{III.33}$$

which apparently converges, as was shown in (III.29).

The Wigner function $W_1^{(S)}(\xi_1')$ characterizing the successfully subtracted state in up to S iteration steps, defined in (III.16) in the structure of a function series, therefore converges uniformly. □

C Evolution of the variance matrix

It is also illustrative to investigate the behavior of the sequence (III.11), which is used to determine the variance matrix of the unsuccessfully subtracted state produced in each iteration step.

The sequence (III.11) defined in the positional form

$${}^{(S)}\nu = \frac{1}{2} + \frac{\zeta^S\left(2\,{}^{(0)}\nu - 1\right)}{2 + \eta\left(1-\zeta^S\right)\left(2\,{}^{(0)}\nu - 1\right)} \tag{III.34}$$

depends on a couple of parameters — the transmittance ζ of a beam splitter realizing the subtraction of a single photon and the efficiency η of an inefficient avalanche photodiode introduced in (II.9). Both the parameters are constrained by the nature of the underlying physical operations to

$$\zeta \in (0,1)\;, \quad \eta \in (0,1)\;. \tag{III.35}$$

It is possible to rewrite the second summand in the relation (III.34) into

$$\underbrace{\frac{\zeta^S}{2 + \eta\left(1-\zeta^S\right)\chi}}_{\varphi_S}\chi = \varphi_S\chi\,, \tag{III.36}$$

with the substitution $\chi \coloneqq \left(2\,{}^{(0)}\nu - 1\right)$. The multiplicative factor φ_S clearly satisfies the $0 \leq \varphi_S \leq \zeta^S\ \forall\, S \in \mathbb{N}$ inequality, which is exploited to show $\varphi_S\chi \to 0$ in the

chain of implications

$$\begin{aligned} \zeta \in (0,1) &\implies \lim_{S\to\infty} \zeta^S = 0 \\ &\implies \lim_{S\to\infty} \varphi_S = 0 \\ &\implies \lim_{S\to\infty} \varphi_S \chi = 0 \\ &\implies \lim_{S\to\infty} {}^{(S)}\nu = 2^{-1}\,, \end{aligned} \tag{III.37}$$

which clearly shows ${}^{(S)}\sigma_1^\circ = \mathrm{diag}\left({}^{(S)}\nu_1, {}^{(S)}\nu_2\right) \to \mathrm{diag}\left(2^{-1}, 2^{-1}\right)$.

The variance matrix ${}^{(S)}\sigma_1^\circ$ of the unsuccessfully subtracted state, defined by the relation (III.11), therefore converges to the variance matrix $\mathrm{diag}\left(2^{-1}, 2^{-1}\right)$ of a vacuum state in the course of the iterative procedure. □

Moreover the sequence (III.11) is strictly monotone. Whether the sequence is actually monotonically increasing or decreasing depends on the value of the first element ${}^{(0)}\nu$. Following (III.11), the difference

$${}^{(S+1)}\nu - {}^{(S)}\nu = -\zeta^S \underbrace{\left(\frac{[1-\zeta]\,[1+\eta\chi]}{[2+\eta\,(1-\zeta^S)\,\chi]\,[2+\eta\,(1-\zeta^{S+1})\,\chi]} \right)}_{\varphi_S} \chi\,, \tag{III.38}$$

where $\chi \coloneqq \left(2\,{}^{(0)}\nu - 1\right)$ is substituted again. The inequality $\varphi_S > 0\;\forall\, S \in \mathbb{N}$ holds as each bracketed expression comprising the φ_S is positive due to the constraints set in (III.35). The sign of the difference ${}^{(S+1)}\nu - {}^{(S)}\nu$ depends solely on the sign of χ.

There are two separate branches of the sequence, the first one is monotonically increasing, while the other one is monotonically decreasing

$${}^{(S+1)}\nu > {}^{(S)}\nu \quad \forall\, {}^{(0)}\nu \in \left(0, 2^{-1}\right)\,, \qquad {}^{(S+1)}\nu < {}^{(S)}\nu \quad \forall\, {}^{(0)}\nu \in \left(2^{-1}, \infty\right)\,, \tag{III.39}$$

where the symbol ν represents both the diagonal elements of ${}^{(S)}\sigma_1^\circ$. □

Chapter IV

Subtraction of a single photon from a mode of light in a squeezed vacuum state

Effects of the subtraction procedure on arbitrary squeezed vacuum states of light are studied through the course of this chapter. The states in consideration are completely described by the variance matrix

$$ {}^{(0)}\sigma_1^\circ = \mathrm{diag}\left(\frac{1}{2}\gamma + \omega, \frac{1}{2}\gamma^{-1} + \omega\right) , \tag{IV.1} $$

where the factor γ defined the gain of the squeezing operation and the parameter ω characterizes the amount of thermal noise, manifested in the form of an additional variance of the quadratures. The parameters γ and ω satisfy

$$ 1 < \gamma\,, \quad 0 \leq \omega\,, \tag{IV.2} $$

with the former condition arising from the assumption of the state being squeezed in the second quadrature variable (p) and the latter condition follows the thermal nature of the noise. Were the condition $0 < \gamma < 1$ to hold, the state would be squeezed in the first and anti–squeezed in the second quadrature variable (x) instead.

The original single step (chapter II) and the iterative (chapter III) single photon

subtraction procedures are compared to each other in terms of the overall probability of success (III.15), (III.28) and the quality of the resulting state (III.17), assessed using the negativity of the central point

$$N^{(S)} = W_1^{(S)}(0,0) \ , \tag{IV.3}$$

of the resulting non–Gaussian Wigner function (III.17). The negativity is generally deemed a suitable measure of the transformation quality [9], as the central point of the initial Gaussian Wigner function of the signal mode in consideration is strictly positive

$$G\left(0, {}^{(0)}\sigma_1^{\circ}\right) > 0 \tag{IV.4}$$

and negative values of $N^{(S)}$ therefore indicate a successful transformation into a non–Gaussian state.

1 Probability and negativity assessment

Both the single step and the iterative procedures are parametrized by the efficiency η of the avalanche detector and the transmittance ζ of the beam splitter used to realize the subtraction. The former parameter η is usually predetermined by the physical properties of the detection apparatus, while the latter parameter ζ may be in principle set to any suitable value with arbitrary precision, allowing the procedure to be fine tuned with optimal performance in mind.

Following that the value of ζ is close to 1 due to the nature of the procedure, it is only reasonable to express both the $N^{(S)}$ (IV.3) and $Q^{(S)}$ (III.28) as functions of the reciprocal reflectivity τ instead of transmittance ζ, yielding the substitution $\zeta = 1 - \tau^2$.

The negativity $N^{(S)}$ and overall probability $Q^{(S)}$ are presented in Figure IV.1 as functions of reflectivity τ on a logarithmic scale for $S = 1, 10, 100, 1000$ iteration steps with the assumption of an ideal detection efficiency $\eta = 1$ and a noiseless $\omega = 0$ squeezed vacuum state $\gamma = 12$.

As the number of iteration steps S increases, the overall probability $Q^{(S)}$ attains its maximal value (III.29) for lower values of τ, permitting a subtraction resulting in the maximal attainable negativity with the maximal achievable probability of

success.

For instance, it is nearly impossible ($Q^{(1)} \approx 0.00025$) to attain the maximal negativity $N \approx -\pi^{-1}$ in the case of the single step subtraction, however, it may be obtained with the maximal probability ($Q^{(42000)} \approx 0.467$) in $S = 42000$ steps.

The negativity $N^{(S)}$ remains mostly unchanged with increasing S; it slightly deepens for higher values of τ before reaching a pointwise limit in respect to S.

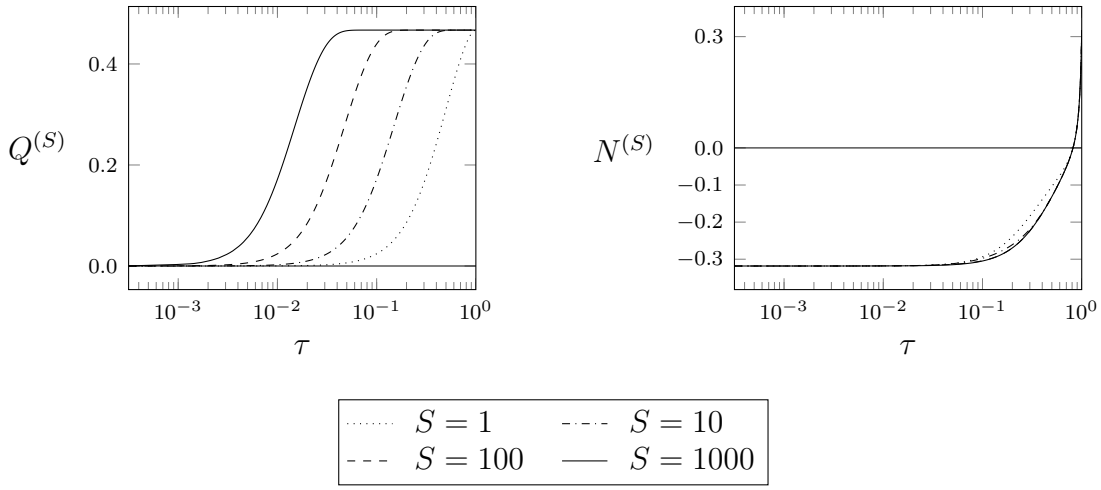

Figure IV.1: The overall probability $Q^{(S)}$ of successful subtraction and the negativity $N^{(S)}$ are displayed as functions of reflectivity τ on a logarithmic scale. The subtraction procedure utilizes an ideal avalanche photodiode ($\eta = 1$) and the signal mode is prepared in a noiseless ($\omega = 0$) squeezed ($\gamma = 12$) vacuum state.

With the increasing number ($S = 1, 10, 100, 1000$) of iteration steps the performance of the procedure improves, as the overall probability $Q^{(S)}$ reaches its limit for lower values of τ, which in turn allows for a subtraction resulting in maximal attainable negativity with the maximal achievable probability of success.

A General comparison of the single step and the iterative subtraction procedures

It would be illustrative to display the relation between $Q^{(S)}(\zeta)$ and $N^{(S)}(\zeta)$ directly, that is to derive the function $N^{(S)}\left(Q^{(S)}\right)$, which can be readily done with

an inverse $\left[Q^{(S)}\right]^{-1}$

$$N^{(S)}(\zeta) = N^{(S)}\left(\left[Q^{(S)}\right]^{-1}\left(Q^{(S)}\right)\right). \tag{IV.5}$$

If the function $Q^{(S)}(\zeta)$ was strictly monotone $\forall\, S \in \mathbb{N}$ it would be also invertible [25]. It is clearly monotone for different values of S in Figure IV.1, however, a more rigorous test is required to establish the function is indeed monotone $\forall\, S \in \mathbb{N}$. The function $Q^{(S)}(\zeta)$ is therefore differentiated in respect to ζ, yielding the fraction

$$\begin{aligned}\frac{\partial Q^{(S)}(\zeta)}{\partial \zeta} &= \frac{\partial}{\partial \zeta}\left[1 - \frac{2}{\sqrt{\det\left[2\mathbb{I} + \eta\left(1-\zeta^S\right)\left(2\,{}^{(0)}\sigma_1^\circ - \mathbb{I}\right)\right]}}\right] \\ &= -2S\eta\zeta^{S-1}\frac{\alpha+\beta+\alpha\beta\left(1-\zeta^S\right)^2}{\sqrt{\left[\left(2+\left(1-\zeta^S\right)\alpha\right)\left(2+\left(1-\zeta^S\right)\beta\right)\right]^3}},\end{aligned} \tag{IV.6}$$

with the substitutions $\alpha = (2\omega - 1 + \gamma)\,\eta$ and $\beta = (2\omega - 1 + \gamma^{-1})\,\eta$. While the denominator in the fraction is clearly positive, it is necessary to establish the numerator is never zero. Expansion of the α and β in the numerator yields

$$\begin{aligned}0 < \frac{(\gamma-1)^2}{\gamma}\left(\left[1-\left(1-\zeta^S\right)^2\eta\right]\eta + 2\omega\left(1-\zeta^S\right)^2\eta^2\right) + \\ 4\omega\eta + 4\omega^2\left(1-\zeta^S\right)^2\eta^2\end{aligned} \tag{IV.7}$$

for parameters γ and ω satisfying the conditions (IV.2). Following that both the numerator and denominator are positive, the first differential itself is negative

$$\frac{\partial Q^{(S)}(\zeta)}{\partial \zeta} < 0 \tag{IV.8}$$

and the $Q^{(S)}(\zeta)$ is therefore a monotonically decreasing function, implying $Q^{(S)}(\zeta)$ is indeed invertible. Because the substitution $\zeta = 1-\tau^2$ was used in the figure Figure IV.1, the $Q^{(S)}(1-\tau^2)$ appears to be a monotonically increasing function of τ

as clearly

$$\begin{aligned}\frac{\partial Q^{(S)}\left(1-\tau^2\right)}{\partial\tau} &= \frac{\partial Q^{(S)}(\zeta)}{\partial\zeta}\frac{\partial\zeta}{\partial\tau} = \frac{\partial Q^{(S)}(\zeta)}{\partial\zeta}\frac{\partial}{\partial\tau}\left(1-\tau^2\right) \\ &= -2\tau\frac{\partial Q^{(S)}(\zeta)}{\partial\zeta} > 0\,.\end{aligned} \tag{IV.9}$$

The convenience of the mapping $N^{(S)}\left(Q^{(S)}\right)$ arises from the comparison of the single step and the iterative procedure presented in the figure Figure IV.2, where the negativity $N^{(S)}$ of the successfully subtracted state in up to $S = 1, 10, 100$ and 1000 iteration steps is shown as a function of the success probability $Q^{(S)}$ for both ideal ($\eta = 1$) and inefficient avalanche photodiode ($\eta = 0.6$).

The iterative procedure outperforms the single step ($S = 1$) subtraction as in general the attained values of negativity $N^{(S)}$ are higher in magnitude with increasing number of iteration steps S for arbitrary values of the probability $Q^{(S)}$.

For example if the procedures ($\eta = 1$) are tuned to yield $N^{(S)} = -0.2$, the success probability increases approximately 3.6× from $Q^{(1)} \approx 0.13$ to $Q^{(1000)} \approx 0.47$. Similarly for a given probability $Q = 0.4$, the negativities $N^{(1)} \approx -0.046$ and $N^{(1000)} \approx -0.247$ are obtained, yielding approximately a 5.4× improvement over the single step procedure.

Moreover, the single step procedure might not yield any negativity at all for higher probabilities, rendering the single step procedure unsuccessful at producing a suitable non–Gaussian state efficiently.

The maximal attainable probability is in both the single and iterative procedures fundamentally bound by the value of (III.29), which depends only on the initial variance ${}^{(0)}\sigma_1^\circ$ and the detection efficiency η. In principle there exist sufficiently squeezed vacuum states ($\gamma \to \infty$)

$$\lim_{\gamma\to\infty}\lim_{S\to\infty} Q^{(S)} = 1 - \frac{2}{\sqrt{\lim\limits_{\gamma\to\infty}\left(2-\eta+2\eta\omega\right)\eta\gamma}} = 1\,, \tag{IV.10}$$

for which the overall probability $Q^{(S)}$ reaches 1.

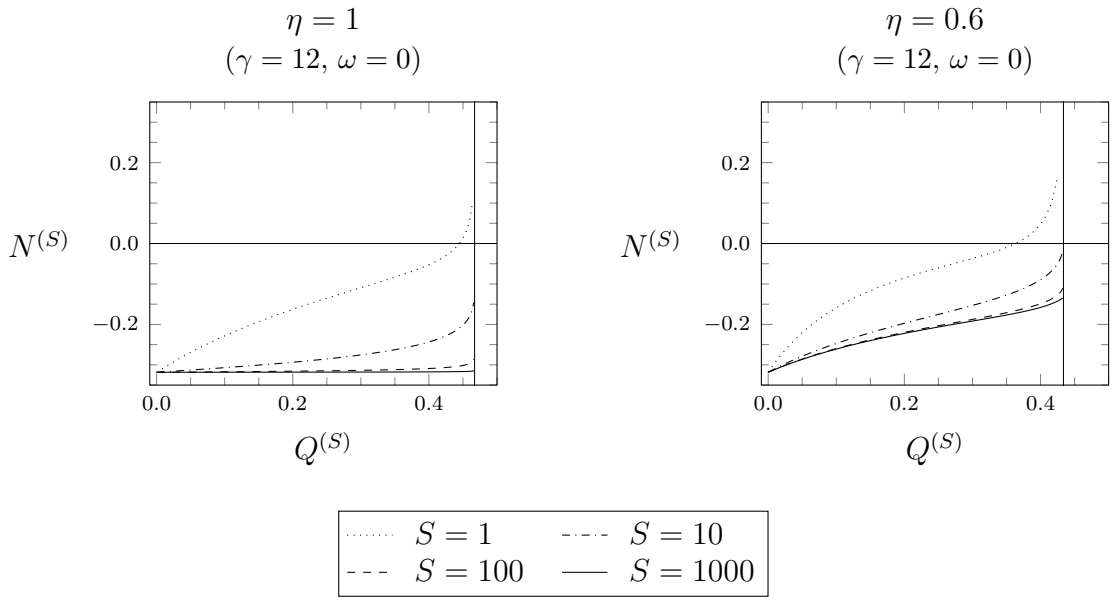

Figure IV.2: The negativity $N^{(S)}$ is displayed as a function of $Q^{(S)}$ for different values of $S = 1, 10, 100, 1000$ using both the ideal and inefficient avalanche photodiode in the procedure. The signal mode is prepared in a noiseless ($\omega = 0$) squeezed ($\gamma = 12$) vacuum state.

B Local minimum of negativity with noisy signal modes

The effects of both subtraction procedures on noiseless squeezed vacuum states were discussed so far. In a more realistic scenario, however, a presence of an additional thermal noise has to be taken into account.

In genral the achievable negativity is reduced with the introduction of the thermal noise. However, a local minimum (a dip) of $N^{(S)}$ is observed in Figure IV.3. The position of the minimum is shifted to the left with higher values of S, i.e., the dip is attained for lower values of τ.

Similarly to Figure IV.1, the negativity slightly improves with increasing number of iteration steps S. The overall probability $Q^{(S)}$ of a successful subtraction behaves equally to the noiseless case; the only difference lies in the value of upper boundary (III.29) arising from the additional noise.

The local minimum of negativity (IV.3) is closely tied to the convergence rate of the underlying series, more precisely to the convergence rate of the series (III.17).

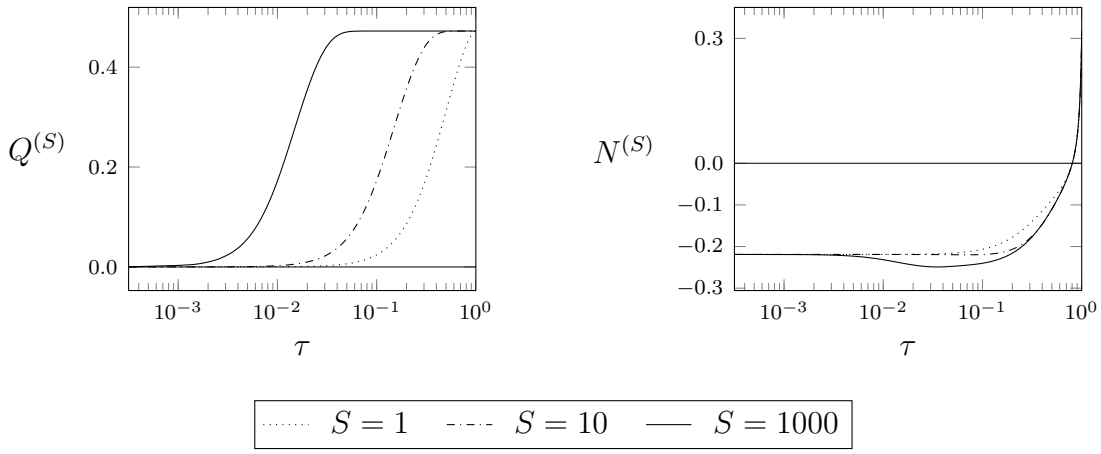

Figure IV.3: Both the overall probability $Q^{(S)}$ of a successful subtraction and the negativity $N^{(S)}$ are displayed as functions of reflectivity τ on a logarithmic scale. The subtraction procedure utilizes an ideal avalanche photodiode ($\eta = 1$) and the signal mode is prepared in a noisy ($\omega = 0.01$) squeezed ($\gamma = 12$) vacuum state.

A local minimum of negativity $N^{(S)}$ is observed for higher numbers of iteration steps.

The relation (IV.3) may be reduced into series

$$N^{(S)} = \frac{2\,\pi^{-1}}{Q^{(S)}} \sum_{Z=1}^{S} \frac{1}{\sqrt{\det\left[2 + \chi\left(\varphi_{Z-1} + 2\,\zeta^{Z}\right)\right]}} - \frac{1}{\sqrt{\det\left[2 + \chi\left(\varphi_{Z} + 2\,\zeta^{Z}\right)\right]}}\,, \tag{IV.11}$$

where the factor $\chi = 2\,{}^{(0)}\sigma_1^{\circ} - 1$ follows the initial variance matrix (IV.1) and the factor $\varphi_Z = \eta\left(1 - \zeta^{Z}\right)$. The series $N^{(S)}$ has been shown to converge in the subsection III.2.B. As an implication, the underlying sequence converges to 0. The convergence rate of the sequence then determines the number of significant summands in (IV.11).

The convergence rate depends on the value of $\zeta = 1 - \tau^2$, which is demonstrated in Figure IV.4, where the elements of the series are shown for different values of τ. In particular, the value $\tau = 10^{-1.5}$ is chosen as it roughly corresponds to the position of a local minimum of negativity attained in up to $S = 1000$ steps.

It is clear from Figure IV.4 that the number of significant summands in (IV.11) considerably increases for lower values of τ. The increase is most noticeable for

values of τ close to the position of the local minimum of $N^{(S)}$.

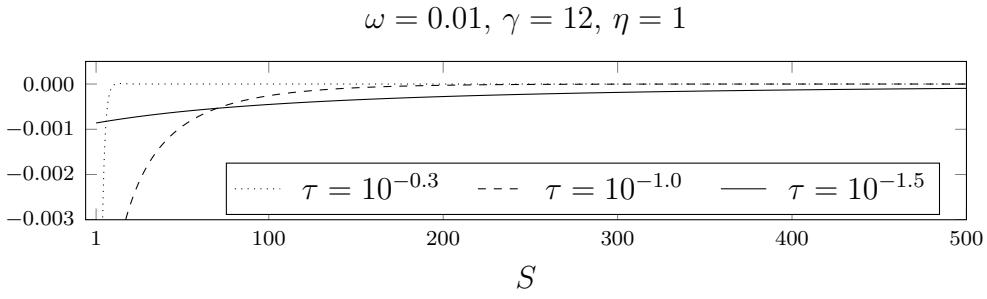

Figure IV.4: Individual elements of the negativity series (IV.11) are displayed for different values of τ.

The subtraction procedure utilizes an ideal avalanche photodiode ($\eta = 1$) and the signal mode is prepared in a noisy ($\omega = 0.01$) squeezed vacuum state ($\gamma = 12$).

Furthermore, the existence of the local minimum of $N^{(S)}$ may be explained with the aid of Figure IV.5, where the negativity of individual Wigner functions of successfully subtracted states (III.14) is presented along with the conditional probability of a successful subtraction (III.13) for different values of τ, chosen to represent the points surrounding the local minimum (for $S = 1000$) in Figure IV.3.

The presence of the thermal noise ($\omega > 0$) prevents the negativity from ever reaching its maximal value

$$ {}^{(S)}W_1^{\bullet}(0,0) > -\pi^{-1} \quad \forall\, S \in \mathbb{N}\,. \tag{IV.12} $$

Each subsequent unsuccessful subtraction attempt reduces the energy of the state: on one hand, the squeezing gain is decreased in this process, but on the other hand so is the noise. The rate at which the gain and noise are reduced is different and after a certain number of iterations, the noise component in the variance (III.11) becomes significant in comparison to the squeezed vacuum until it finally converges to $\mathrm{diag}\,(2^{-1}, 2^{-1})$. Consequently the negativity of the Wigner function (III.14) decreases.

Moreover, only a limited number of iterations has any effect on the total negativity, as the weighing factor ${}^{(S)}P_{\bullet}$ presented in Figure IV.5 converges to zero. For instance the ${}^{(S)}P_{\bullet}\,(\tau = 10^{-0.3})$ converges in mere 15 iteration steps, while the ${}^{(S)}P_{\bullet}\,(\tau = 10^{-1.5})$ converges in over 1000 steps.

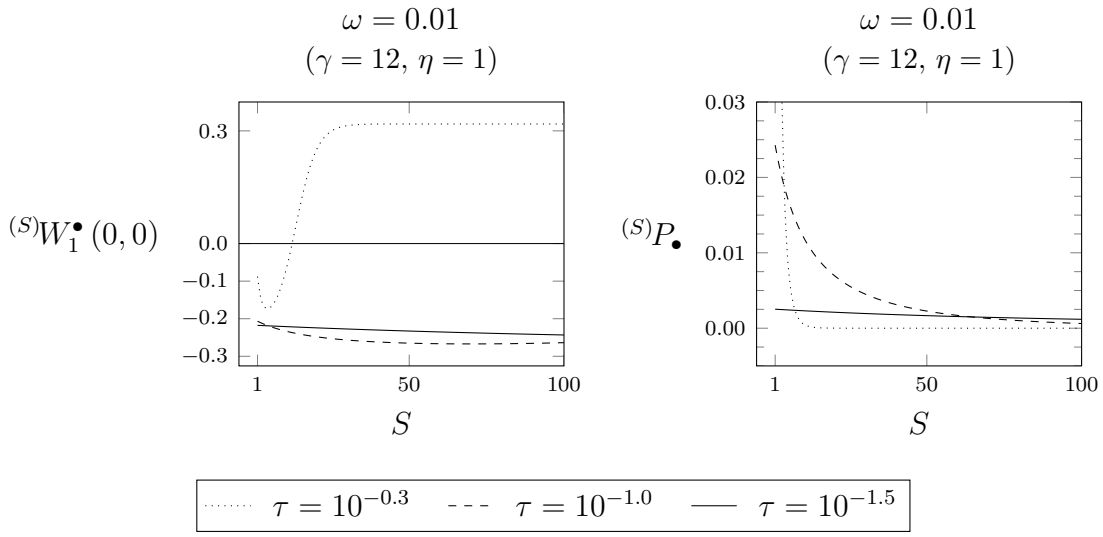

Figure IV.5: The negativities of individual Wigner functions (III.14) is displayed along the probability (III.13) for different values of τ. The subtraction procedure utilizes an ideal avalanche photodiode ($\eta = 1$) and the signal mode is prepared in a noisy ($\omega = 0.01$) squeezed vacuum state ($\gamma = 12$).

The strength of the effects of both procedures in the ideal detection regime $\eta = 1$ on noisy signal modes is presented in Figure IV.6 with each plot pertaining to a different level of noise ω, e.g., 2, 5, 10 and 20 percent of vacuum fluctuations. The presence of the local minimum (dip) is manifested by the decreasing tendency of the negativity.

The importance of the existence of local minimum arises from the observation that the minimum of $N^{(S)}$ occurs close to the upper boundary of probability $Q^{(S)}$, implying it is possible to fine tune the iterative subtraction to perform optimally even with noisy signal modes.

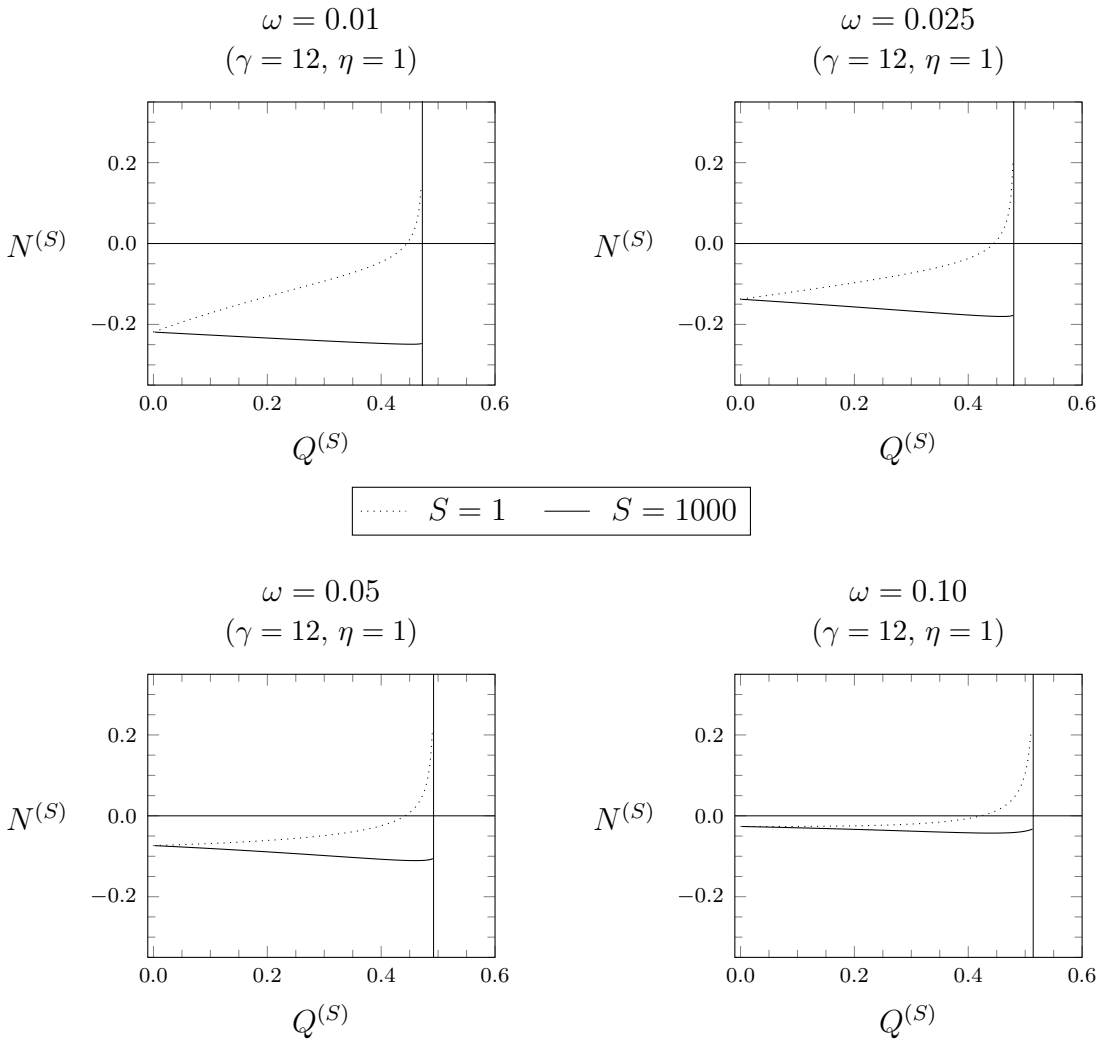

Figure IV.6: The negativity $N^{(S)}$ is displayed as function of probability $Q^{(S)}$ for different values of S. The procedure is assumed to be working in the ideal detection regime ($\eta = 1$). The signal modes are prepared in a noisy squeezed ($\gamma = 12$) vacuum states with the additional noise taking the values of $\omega = 0.01, 0.025, 0.05, 0.10$.

The presence of the local minimum (dip) is manifested by the decreasing tendency of the negativity until it reaches a local minimum in respect to $Q^{(S)}$ located near the maximal achievable value given by (III.29).

Unfortunately, the local minimum slowly ceases to exist when the inefficient detection is considered, as is shown in Figure IV.7 for $\eta = 0.91, 0.60$. Notably, it is possible to counter the inefficient detection with strongly squeezed states to some extent.

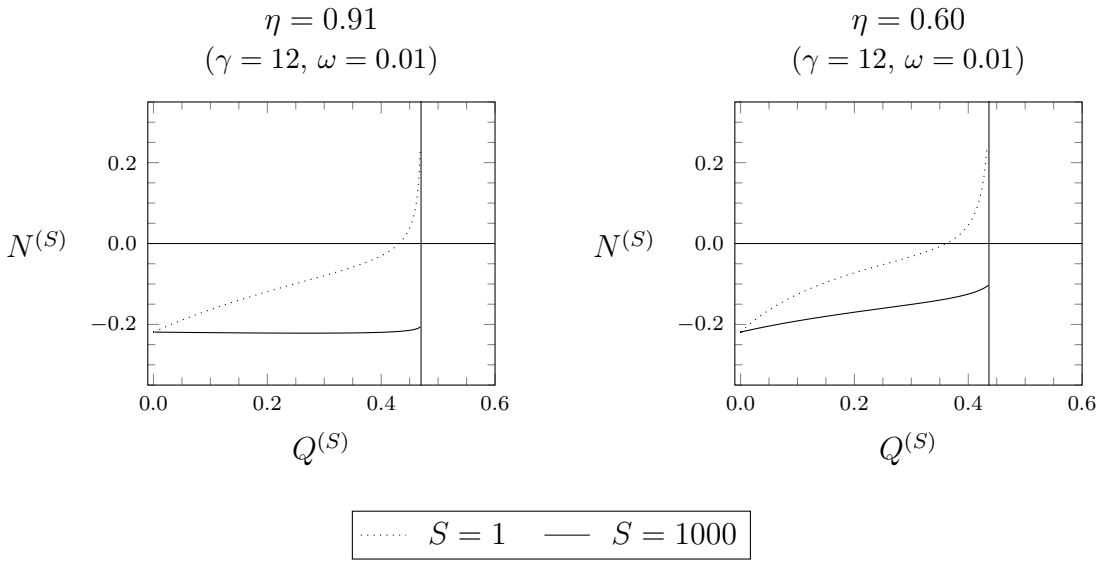

Figure IV.7: The negativity $N^{(S)}$ is displayed as function of probability $Q^{(S)}$ for different values of S. The procedure is assumed to be working in the inefficient detection regime ($\eta = 0.91, 0.60$). The signal modes are prepared in a noisy ($\omega = 0.01$) squeezed ($\gamma = 12$) vacuum state.

The local minimum (dip) previously manifested by the decreasing tendency of the negativity disappears with lower detection efficiencies.

2 Optimization of negativity

In practice only a single parameter characterizing the single step procedure may be arbitrarily manipulated, i.e., the transmittance $\zeta = 1 = \tau^2$ of the beam splitter used to tap the light off. The iterative procedure is characterized by an additional parameter, as it either succeeds in up to S iteration steps or exceeds the number of attempts and fails.

The relation between the number of iteration steps S and the overall probability of success and negativity was shown in the subsection IV.1.A, indicating higher numbers of iteration steps generally lead to better performance. These indications were extended in the subsection IV.1.B with the observation of a local minimum in negativity occurring when subtracting from noisy states. The presence of the local minimum suggested that fine tuning of the procedure was possible.

It is therefore only natural to search for optimal values of $\tau^{(S)}$ resulting in both

the maximal negativity N^S and preferably also maximal attainable probability Q^S of a successful subtraction for different values of S.

The optimal values of $\tau^{(S)}$, along with the resulting negativity N^S and the overall probability of a successful subtraction Q^S are presented in Figure IV.8. The optimization is performed with only the maximal negativity in mind, resulting in a slightly lower probabilities Q^S than the maximally attainable one given by the relation (III.29).

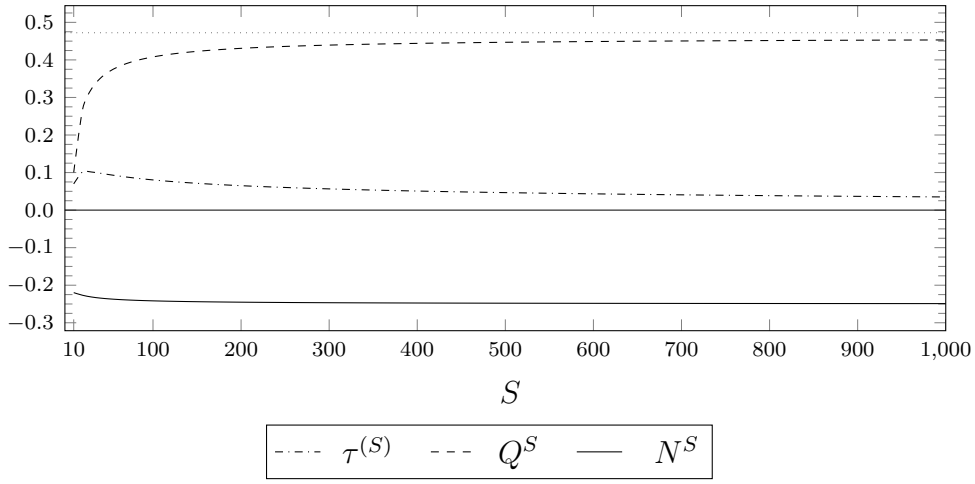

Figure IV.8: The optimization of the procedure working in the ideal detection regime ($\eta = 1$) is performed with only the maximal negativity in mind. The optimal values of $\tau^{(S)}$, along with the resulting negativity N^S and the overall probability Q^S are shown in the plot for increasing number of iteration steps S for a noisy ($\omega = 0.01$) squeezed ($\gamma = 0.01$) vacuum state.

The upper straight dotted line represents the upper boundary (maximal value) of the overall probability.

Conclusions and outlooks

The iterative subtraction procedure, proposed in chapter III, was analyzed in chapter IV. It surpassed the single step subtraction procedure when applied to squeezed vacuum states, as the signal was transformed into maximally non–Gaussian states with considerably higher probability of success. The iterative procedure produced non–Gaussian states in situations where the single step procedure could not, e.g., noisy signal modes and inefficient avalanche photodiodes.

The current analysis of the proposed iterative procedure in terms of negativity is, however, only a first step in a long flight of stairs. First of all it would be enlightening to include purity and overlap with the initial state in the current analysis. Secondly, the optimization strategy could perhaps profit from adoptive tuning of the transmittance in each step of the iteration; this idea may be put to to test in further research. Moreover, the model of the subtraction may be extended to account for more general Gaussian states, i.e., states with non–zero vector of mean values.

Bibliography

[1] Weedbrook, C., Pirandola, S., García-Patrón, R., Cerf, N. J., Ralph, T. C., Shapiro, J. H., and Lloyd, S. "Gaussian quantum information". In: *Rev. Mod. Phys.* 84 (2 May 2012), pp. 621–669. DOI: 10.1103/RevModPhys.84.621 (Cited on pages 4, 6, 10–12).

[2] Lloyd, S. and Braunstein, S. L. "Quantum Computation over Continuous Variables". In: *Phys. Rev. Lett.* 82 (8 Feb. 1999), pp. 1784–1787. DOI: 10.1103/PhysRevLett.82.1784 (Cited on pages 4, 10).

[3] Giedke, G. and Ignacio Cirac, J. "Characterization of Gaussian operations and distillation of Gaussian states". In: *Phys. Rev. A* 66 (3 Sept. 2002), p. 032316. DOI: 10.1103/PhysRevA.66.032316 (Cited on page 4).

[4] Braunstein, S. L. and Loock, P. van. "Quantum information with continuous variables". In: *Reviews of Modern Physics* 77 (2 June 2005), pp. 513–577. DOI: 10.1103/RevModPhys.77.513 (Cited on pages 4, 6, 9).

[5] Lvovsky, A. I. and Mlynek, J. "Quantum-Optical Catalysis: Generating Nonclassical States of Light by Means of Linear Optics". In: *Phys. Rev. Lett.* 88 (25 June 2002), p. 250401. DOI: 10.1103/PhysRevLett.88.250401 (Cited on page 4).

[6] Yukawa, M., Miyata, K., Mizuta, T., Yonezawa, H., Marek, P., Filip, R., and Furusawa, A. "Generating superposition of up-to three photons for continuous variable quantum information processing". In: *Opt. Express* 21.5 (Mar. 2013), pp. 5529–5535. DOI: 10.1364/OE.21.005529 (Cited on page 4).

[7] Zavatta, A., Viciani, S., and Bellini, M. "Quantum-to-Classical Transition with Single-Photon-Added Coherent States of Light". In: *Science* 306.5696 (2004), pp. 660–662. DOI: 10.1126/science.1103190 (Cited on page 4).

[8] Parigi, V., Zavatta, A., Kim, M., and Bellini, M. "Probing Quantum Commutation Rules by Addition and Subtraction of Single Photons to/from a Light Field". In: *Science* 317.5846 (2007), pp. 1890–1893. DOI: 10.1126/science.1146204 (Cited on page 4).

[9] Wenger, J., Tualle-Brouri, R., and Grangier, P. "Non–Gaussian Statistics from Individual Pulses of Squeezed Light". In: *Physical Review Letters* 92 (15 Apr. 2004), p. 153601. DOI: 10.1103/PhysRevLett.92.153601 (Cited on pages 4, 13, 15, 38).

[10] Kim, M. S., Park, E., Knight, P. L., and Jeong, H. "Nonclassicality of a photon-subtracted Gaussian field". In: *Physical Review A* 71 (4 Apr. 2005), p. 043805. DOI: 10.1103/PhysRevA.71.043805 (Cited on pages 4, 13).

[11] Ourjoumtsev, A., Dantan, A., Tualle-Brouri, R., and Grangier, P. "Increasing Entanglement between Gaussian States by Coherent Photon Subtraction". In: *Physical Review Letters* 98 (3 Jan. 2007), p. 030502. DOI: 10.1103/PhysRevLett.98.030502 (Cited on pages 4, 13).

[12] Zavatta, A., Parigi, V., Kim, M. S., and Bellini, M. "Subtracting photons from arbitrary light fields: experimental test of coherent state invariance by single-photon annihilation". In: *New Journal of Physics* 10.12 (2008), p. 123006. DOI: 10.1088/1367-2630/10/12/123006 (Cited on pages 4, 13).

[13] Dirac, P. A. M. "A new notation for quantum mechanics". In: *Mathematical Proceedings of the Cambridge Philosophical Society* 35 (03 July 1939), pp. 416–418. ISSN: 1469-8064. DOI: 10.1017/S0305004100021162 (Cited on page 5).

[14] Adesso, G., Ragy, S., and Lee, A. R. "Continuous Variable Quantum Information: Gaussian States and Beyond". In: *Open Systems and Information Dynamics* 21.01n02 (2014), p. 1440001. DOI: 10.1142/S1230161214400010 (Cited on pages 6–12, 15).

[15] Leonhardt, U. *Measuring the Quantum State of Light*. Cambridge Studies in Modern Optics. Cambridge University Press, 1997. ISBN: 9780521497305 (Cited on pages 6–10, 12).

[16] Sakurai, J. J. *Modern quantum mechanics*. Harlow, Essex: Pearson, 2014. ISBN: 9781292024103 (Cited on pages 7, 9).

[17] Greiner, W. *Thermodynamics and statistical mechanics*. New York: Springer-Verlag, 1995. ISBN: 978-0-387-94299-5 (Cited on page 7).

[18] Kolmogorov, A. N. *Foundations of the theory of probability*. New York: Chelsea publishing company, 1956 (Cited on page 7).

[19] Wigner, E. "On the Quantum Correction For Thermodynamic Equilibrium". In: *Physical Review Letters* 40 (5 June 1932), pp. 749–759. DOI: 10.1103/PhysRev.40.749 (Cited on page 7).

[20] Yu, Z.-s., Ren, G.-h., Fan, H.-y., Cai, G.-C., and Jiang, N.-Q. "Fock-Space Projector Studied in Weyl Ordering Approach". English. In: *International Journal of Theoretical Physics* 51.7 (2012), pp. 2256–2261. ISSN: 0020-7748. DOI: 10.1007/s10773-012-1105-y (Cited on page 10).

[21] Abramowitz, M. *Handbook of mathematical functions: with formulas, graphs, and mathematical tables*. New York: Dover Publications, 1970. ISBN: 978-0486612720 (Cited on page 10).

[22] García-Patrón, R., Fiurášek, J., Cerf, N. J., Wenger, J., Tualle-Brouri, R., and Grangier, P. "Proposal for a Loophole-Free Bell Test Using Homodyne Detection". In: *Physical Review Letters* 93 (13 Sept. 2004), p. 130409. DOI: 10.1103/PhysRevLett.93.130409 (Cited on page 15).

[23] Yoshikawa, J.-i., Makino, K., Kurata, S., Loock, P. van, and Furusawa, A. "Creation, Storage, and On-Demand Release of Optical Quantum States with a Negative Wigner Function". In: *Phys. Rev. X* 3 (4 Dec. 2013), p. 041028. DOI: 10.1103/PhysRevX.3.041028 (Cited on page 25).

[24] Stewart, J. *Calculus: Early Transcendentals*. Belmont, California: Cengage Learning, 2012. ISBN: 978-0538497909 (Cited on page 34).

[25] Binmore, K. G. *Mathematical analysis: a straightforward approach*. Cambridge New York: Cambridge University Press, 1977. ISBN: 0521291674 (Cited on page 40).